The Role of Retinal Connexins Cx36 and Horizontal Cell Coupling in Emmetropization in Guinea Pigs

Zhina Zhi,[1,2] Jing Xiang,[1,2] Qian Fu,[1,2] Xiaomeng Pei,[1,2] Dengke Zhou,[1,2] Yuqing Cao,[1,2] Liqin Xie,[1,2] Sen Zhang,[1,2] Si Chen,[1,2] Jia Qu,[1,2] and Xiangtian Zhou[1,2]

[1]School of Optometry and Ophthalmology, and Eye Hospital, Wenzhou Medical University, Wenzhou, Zhejiang, China
[2]State Key Laboratory and Key Laboratory of Vision Science, Ministry of Health People's Republic of China and Zhejiang Provincial Key Laboratory of Ophthalmology and Optometry, Wenzhou, Zhejiang, China

Correspondence: Xiangtian Zhou, School of Optometry and Ophthalmology, and Eye Hospital, Wenzhou Medical University, 270 Xueyuan Road, Wenzhou, Zhejiang 325003, People's Republic of China; zxt@mail.eye.ac.cn.

Received: September 17, 2020
Accepted: June 24, 2021
Published: July 20, 2021

Citation: Zhi Z, Xiang J, Fu Q, et al. The role of retinal connexins Cx36 and horizontal cell coupling in emmetropization in guinea pigs. *Invest Ophthalmol Vis Sci.* 2021;62(9):27. https://doi.org/10.1167/iovs.62.9.27

Purpose. The purpose of this study was to determine whether retinal gap junctions (GJs) via connexin 36 (Cx36, mediating coupling of many retinal cell types) and horizontal cell (HC-HC) coupling, are involved in emmetropization.

Methods. Guinea pigs (3 weeks old) were monocularly form deprived (FD) or raised without FD (in normal visual [NV] environment) for 2 days or 4 weeks; alternatively, they wore a −4 D lens (hyperopic defocus [HD]) or 0 D lens for 2 days or 1 week. FD and NV eyes received daily subconjunctival injections of a nonspecific GJ-uncoupling agent, 18-β-Glycyrrhetinic Acid (18-β-GA). The amounts of total Cx36 and of phosphorylated Cx36 (P-Cx36; activated state that increases cell-cell coupling), in the inner and outer plexiform layers (IPLs and OPLs), were evaluated by quantitative immunofluorescence (IF), and HC-HC coupling was evaluated by cut-loading with neurobiotin.

Results. FD per se (excluding effect of light-attenuation) increased HC-HC coupling in OPL, whereas HD did not affect it. HD for 2 days or 1 week had no significant effect on retinal content of Cx36 or P-Cx36. FD for 4 weeks decreased the total amounts of Cx36 and P-Cx36, and the P-Cx36/Cx36 ratio, in the IPL. Subconjunctival 18-β-GA induced myopia in NV eyes and increased the myopic shifts in FD eyes, while reducing the amounts of Cx36 and P-Cx36 in both the IPL and OPL.

Conclusions. These results suggest that cell-cell coupling via GJs containing Cx36 (particularly those in the IPL) plays a role in emmetropization and form deprivation myopia (FDM) in mammals. Although both FD and 18-β-GA induced myopia, they had opposite effects on HC-HC coupling. These findings suggest that HC-HC coupling in the OPL might not play a significant role in emmetropization and myopia development.

Keywords: gap junctions, Cx36, horizontal cells, Cx57/Cx50, myopia

Myopia prevalence has increased dramatically over the last three decades – especially in East Asia, where the prevalence of myopia reached 47% in 2010 and is predicted to soar to 65.3% in 2050.[1] This rapid increase in myopia prevalence is very likely due to environmental changes in modern life – especially changes in visual environment, as supported by evidence from both animal research and human epidemiological studies. Abnormal visual environments – blurring of retinal images, due to imposed form deprivation (FD) or hyperopic defocus (HD) – induce myopia in animal models, including chicks and guinea pigs,[2,3] and spending longer time outdoors decreases children's risk of developing myopia.[4] Therefore, emmetropization – the regulated development of ocular growth, so as to establish a match between the axial growth and optical development of the eye – is guided by visual input.

The retina is a thin layer of neural tissue that receives and processes light-stimuli, and regulates axial elongation via signals transmitted to the sclera through the retinal pigment epithelium (RPE) and choroid. Light-dependent changes in photoreceptor activity are transmitted to retinal ganglion cells via circuits containing electrical synapses (gap junctions [GJs]) as well as chemical synapses.[5] GJs are transmembrane conduits between two cells, composed of connexin (Cx) subunits, which mediate the regulated passage of small molecules and ions between the coupled cells.[6,7] They are involved in multiple myopia-related retinal functions, including light adaptation,[8,9] neural transmission in the mammalian rod pathway,[10] and the control of contrast sensitivity.[11,12] Of particular interest, dopamine,[13] nitric oxide,[14] and retinoic acid,[15] retinal signaling agents that are known to play roles in emmetropization, also have been shown to dynamically regulate cell-cell coupling in the retina via GJs.[11] In the chick, dopamine, nitric oxide, and inhibitors of GJ-mediated coupling, as well as increases in ambient light intensity, increase contrast detection at higher spatial frequencies.[12] Given that spatial detail and contrast are likely to be important for discriminating image focus/defocus, these findings suggest that visual regulation of retinal cell-cell coupling through GJs

might play a significant role in emmetropization and myopia.

Among the 20 different isoforms of GJ proteins (connexins) identified to date,[6] Cx36 and Cx57 in particular are recognized as being abundant in retinas.[16] In mammalian retinas, Cx36, the most prevalent of these,[17,18] plays a critical role in both the primary rod pathway (forming homocellular GJs between AII amacrine cells, and heterocellular GJs between AII amacrines and ON-cone bipolar cells)[17] and in secondary rod pathways (forming GJs between rods and cones).[18,19] Multiple independent investigations, including genomewide association studies (GWAS), have found that the *GJD2* gene (encoding Cx36) is associated with human myopia.[20,21] The eyes of *Gnat1*$^{-/-}$ mice, which lack functional rods but retain photopic vision,[22] do not develop myopia in response to FD[23]; this suggests that Cx36 might affect emmetropization in mammals by regulating rod-pathway functions, although other mechanisms and pathways have not been ruled out. Selective blockade of coupling via GJs containing Cx35 (the chicken orthologue of Cx36) mimics the effect of increasing light intensity in chicks – viz., increasing retinal contrast sensitivity and inhibiting form deprivation myopia (FDM) (Teves M, et al., 2015, the 15th International Myopia Conference; and W.K. Stell, personal communication). Recent studies also have found that FD and HD caused decreased expression of *GJD2* mRNA and Cx36 protein in guinea pig retina.[24,25] In addition, eyelid suture for 40 days was found to increase the level of Cx36 phosphorylation in the mouse retina,[26] indicating that FD increased cell-cell coupling in the retina. Cx57/Cx50 forms GJs exclusively among retinal horizontal cells (HCs) in mice.[8,27] The dynamic regulation of HC-HC coupling during light adaptation affects the center-surround receptive field organization of retinal neurons, as well as retinal contrast detection.[11,12] Degradation of retinal image contrast by FD and HD induces myopia in many species, including chicks, mice, guinea pigs, tree shrews, and monkeys.[28] Thus HC-HC coupling, too, might be involved in the visual regulation of emmetropization.

The guinea pig is a well-established model in myopia research. Guinea pigs are particularly suitable for studying the roles of retinal GJs in myopia, because the distribution of Cx36 in their retinas is similar to that in human retinas[29] and because the avascular retina of guinea pigs is especially advantageous for evaluating HC-HC coupling by the cut-loading technique.[30] To determine whether retinal GJs formed by Cx36 – as well as the GJs responsible for HC-HC coupling – are involved in regulating emmetropization, in the present study, we investigated the effects of FD on the retinal content of Cx36 and P-Cx36, as well as on HC-HC coupling. We also evaluated the effect of subconjunctival injection of a nonspecific GJ-uncoupling agent – 18-β-glycyrrhetinic acid (18-β-GA) – on emmetropization, the content and phosphorylation-state of Cx36, and HC-HC coupling in the retina.

Methods

Animals

The animal research in this study was approved by the Animal Care and Ethics Committee at Wenzhou Medical University, Wenzhou, China. Treatment and care of the animals adhered to the ARVO Statement for the Use of Animals in Ophthalmic and Vision Research (https://www.arvo.org/About/policies/statement-for-the-use-of-animals-in-ophthalmic-and-vision-research/). Pigmented guinea pigs (3 weeks old) were obtained from the Animal Breeding Unit at Wenzhou Medical University. All animals were raised on a cycle of 12 hours of illumination (300 lux, on at 08:00) and 12 hours of darkness throughout the experimental period.

Experimental Design

The time courses of FDM and LIM are different, in guinea pigs as in other animal models of myopia. LIM induced by a −4 D lens can be compensated in 1 week; but FD cannot be compensated, because ocular elongation continues without restraint when visual image details are degraded by a translucent latex diffuser. Thus, the rate and therefore the magnitude of myopia development diminishes over time with HD, but can be sustained during FD.[31–33] For this reason, we evaluated Cx36 content in the OPL and IPL, and HC-HC coupling, after 2 days and 1 week of HD; this allowed us to focus on changes that might be causal in myopization, during 2 distinct phases: (1) the initiating and developing phase of HD compensation (2 days), and (2) the compensated phase of HD (1 week). For FD, we evaluated Cx36 content and HC-HC coupling: (1) after 2 days (initiating and early developing phase, when there are no measurable changes/differences in axial elongation or refractive error), and (2) after 4 weeks (late developed phase) of FD treatment (Fig. 1).

Aim 1: The effects of FD and HD on HC-HC coupling. To evaluate the effect of FD on HC-HC coupling, guinea pigs were monocularly FD ($n = 10$) or raised without FD (in normal visual environment [NV], $n = 8$). To evaluate the effects of decreased illuminance caused by FD, 16 additional animals were raised in NV environment, with illuminance at 300 lux (NV-300 lux, $n = 6$) or 40 lux (NV-40 lux, $n = 10$). To evaluate the effect of HD on HC-HC coupling, animals were divided into 3 groups: NV ($n = 8$), 0 D ($n = 6$), and −4 D ($n = 10$). After 2 days of treatment under 300 lux or 40 lux illumination (same illumination as during the treatment period), HC-HC coupling was evaluated by cut-loading on the third day after light-on for another 1 hour.

Aim 2: The effects of FD and HD on retinal content of Cx36 and P-Cx36. For the HD groups, guinea pigs wore a monocular −4 D or 0 D lens for 2 days (0 D: $n = 5$ and −4 D: $n = 6$) or 1 week (0 D: $n = 7$ and −4 D: $n = 9$). For the FD groups, guinea pigs were monocularly form deprived or raised without FD (NV) for 2 days (NV-300 lux: $n = 7$; NV-40 lux: $n = 7$; and FD: n = 7) or 4 weeks (NV-300 lux: $n = 9$ and FD: $n = 6$). The relative amounts of Cx36 and P-Cx36 were evaluated by quantitative immunofluorescence (IF).

Aim 3: The effects of subconjunctival 18-β-GA on refraction, amounts of Cx36 and P-Cx36, and HC-HC coupling. NV and monocularly FD guinea pigs were raised under 300 lux illumination. All animals were divided into 3 groups – NV into NV + Vehicle ($n = 12$); NV + 18-β-GA, 40 µg ($n = 14$); and NV + 18-β-GA, 120 µg ($n = 13$); – and FD into FD + Vehicle ($n = 17$); FD + 18-β-GA, 40 µg ($n = 18$); and FD + 18-β-GA, 120 µg ($n = 18$). Ocular biometry was performed at weeks 2 and 4 in all groups. HC-HC coupling was evaluated at day 2 in NV ($n = 8$), NV + V ($n = 7$), and NV + 18-β-GA, 120 µg ($n = 8$) groups, and the amounts of Cx36 and P-Cx36 were measured at week 4 in the NV ($n = 6$), NV + V ($n = 7$), and NV + 18-β-GA, 120 µg ($n = 11$) groups.

Investigative Ophthalmology & Visual Science

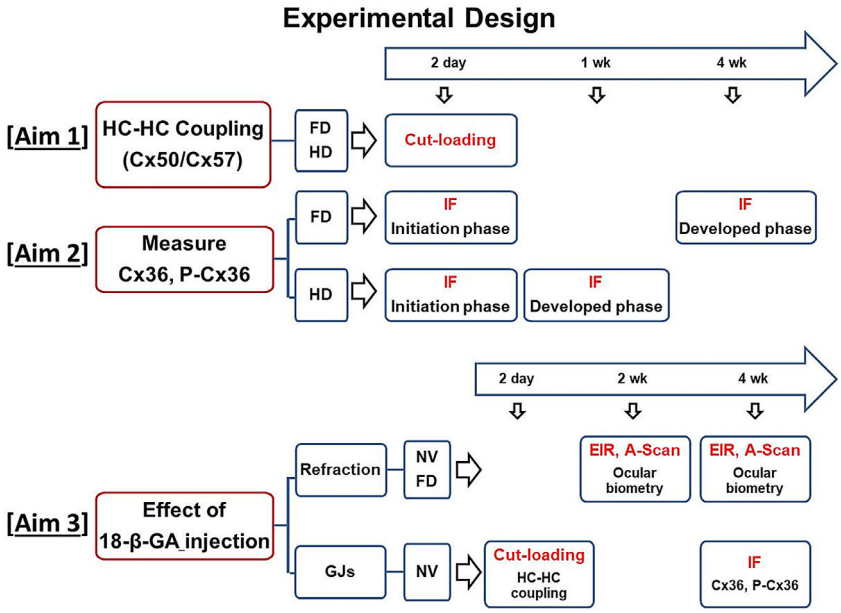

Figure 1. Experimental Design. HC, horizontal cell; FD, form deprivation; HD, hyperopic defocus; NV, normal visual environment; IF, immunofluorescence; GJs, gap junctions; EIR, eccentric infrared retinoscopy.

Establishing the Guinea Pig Myopia Model

Guinea pigs wore translucent latex diffusers over their eyes for 2 days or 4 weeks, to induce FDM.[2] Animals in the HD groups wore, on their right eyes, either a −4 D lens (to induce LIM) or 0 D lens (as a control). The illuminance at the front of the FD eye was 40 lux in the 300 lux environment, as measured with a diffuser over the sensor of a photometer (AS823, Smart sensor, Dongguan, China). Thus, animals in the NV groups were raised under 300 lux or 40 lux (LED, Weiguzhaoming, Wenzhou, China, model number 12v-5630, white light [color temperature: 6000–6500 K]). Illuminance was adjusted to 300 lux or 40 lux by modulating the voltage (and thereby, the current, power supplied in direct current mode) provided for the lights, while measuring with the photometer.

Drug Administration

The sclera of guinea pigs is very thin, approximately 87 ± 11 µm (n = 5, measured in retinal frozen sections), so it cannot be assumed to heal reliably after intravitreal injections. In our experience, the injection site keeps open even one week after injection; therefore, subconjunctival injection is widely used for local drug application to ocular tissues in guinea pigs, even when the targets are located internally (e.g. retina).[34,35] For subconjunctival injections, stock solutions of the gap-junction antagonist, 18-β-GA (G10105; Sigma, Buchs, Switzerland), were prepared by mixing 0.85 mmol or 2.55 mmol 18-β-GA in 60 µL of 100% dimethyl sulfoxide (DMSO; D2650; Sigma) and stored at −20°C until use. These stock solutions were freshly diluted in double-distilled water (ddH_2O), just before use, to achieve the final concentrations designated "low-dose" (85 µM, 40 µg/100 µL) and "high-dose" (255 µM, 120 µg/100 µL) 18-β-GA. In the drug-injection groups, 100 µL of low- or high-dose solution or DMSO vehicle alone was injected subconjunctivally every day for 2 days or 4 weeks, after topical anesthesia with proparacaine hydrochloride eye drops (Alcaine; Alcon, Belgium). We used fine needles (26 or 30 gauge) and minimized injury and drug reflux by avoiding previous injection sites.

Biometric Measurements

Biometric parameters (refraction and axial dimensions) were measured in all animals, 0, 2, and 4 weeks after 18-β-GA injection. These measurements were performed during the daytime by an optometrist who was blinded as to the identity of the treatment group.

The methods of biometric measurements were as described in our previous studies.[31,32] In brief, eccentric infrared retinoscopy (EIR) with custom software was used to measure refraction along the vertical meridian. An A-scan ultrasonograph (11 MHz frequency; Quantel Medical, Aviso, France) was used to measure the length of the axial components of the eye, including anterior chamber depth (ACD), lens thickness (LT), vitreous chamber depth (VCD), and axial length (AL; defined as the distance between the anterior corneal surface and the anterior retinal surface). The conduction velocities for converting measurements of time to length were taken as 1534 m/s for ACD, 1723 m/s for LT, and 1540 m/s for VCD, as described previously.[31,32]

Preparation of the Retina and Immunofluorescence Imaging

Cx36 and P-Cx36 were imaged by immunofluorescence (IF), as described previously.[17,36] The guinea pigs were euthanized by cervical dislocation at 9:00 to 11:00 AM under 300 lux or 40 lux environments (according to the treatment condition), eyes were enucleated and hemisected through the equator, cornea and lens were removed, and the posterior eyecups were fixed at room temperature (25°C) in 2% N′-(3-Dimethylaminopropyl)-N-

Investigative Ophthalmology & Visual Science

ethylcarbodiimide hydrochloride (EDAC; Sigma-Aldrich, Cat. # E6383) in 0.1 M PB (PH = 7.5) for 30 minutes. Fixed tissue was cryoprotected by direct transfer into 30% sucrose, kept for 24 hours at 4°C, embedded in OCT (6505; ThermoFisher, Waltham, MA, USA), and snap-frozen in liquid nitrogen. Eyes were sectioned at 12 µm, parallel to the optic axis and near the center of the retina, and sections were mounted on glass slides coated with polylysine (SLI-20010; Maixin, Fuzhou, China); for immunolabeling, nonspecific binding was blocked by incubating for 2 hours at room temperature with 6% donkey serum (Jackson ImmunoResearch, West Grove, PA, USA) in PBST (PBS [0.1 M phosphate buffer + 0.9% NaCl] + 1% bovine serum albumin [BSA] + 0.2% Triton X-100, pH = 7.4). Sections were then incubated at 4°C overnight with a mixture of mouse anti-Cx36 IgG (MAB3045, EMD Merck, Boston, MA, USA; 1:500), as follows: for the FD groups, after 2 days and 4 weeks; for the HD groups, after 2 days (using lot number 2905342), and after 1 week (using lot number 2990382); and with rabbit anti-Cx36-phospho-Ser293 IgG (a generous gift from Dr. J. O'Brien, The University of Texas; 1:1000) in 6% donkey serum with PBST. Sections were washed 5 times for 7 minutes in PBS, and then incubated at room temperature for 2 hours with a mixture of secondary antibodies: Alexa Fluor555 donkey anti-mouse IgG (A31570, Molecular Probes; 1:400) and Alexa Fluor488 donkey anti-rabbit IgG (A21206, Molecular Probes; 1:400). Cover-slips were applied with Vectashield mounting medium containing DAPI (Vector, USA) to label cell nuclei. Control slides were prepared in which primary antibody had been omitted.

Images were acquired on a laser confocal microscope (Zeiss LSM 710, Göttingen, Germany) with a 63x/NA = 1.5 oil-immersion objective lens; image size: 134.95 µm × 134.95 µm; pixel size: 0.13 µm (x), 0.13 µm (y), and 1.00 µm (z). A z-stack of images was acquired at 2 µm intervals, including the entire depth of the IPL and OPL. The settings were optimized in preliminary trials, and then kept constant for all conditions and treatments so as to avoid imaging biases. Images were taken approximately two to three microscope fields away from the optic nerve head, in both directions (nasally and temporally). Four images were collected from both of two cryosections of one eyecup, and measurements from the eight images were averaged to represent the values for that one animal. The confocal images were analyzed with ImageJ software (National Institutes of Health, USA; https://imagej.nih.gov). Each image was split into two channels, representing the Cx36 and P-Cx36 images. The Cx36 image was first converted into a binary image, with a threshold of 0, and separate, well-imaged regions of the IPL and OPL were chosen for detailed analysis. Cx36-immunoreactive (-IR) puncta were discriminated and analyzed automatically as regions of interest (ROIs), and the fluorescence intensity of Cx36-IR plaques (I_{Cx36}) was estimated by calculating the summed intensities of all ROIs in each image. At the same time, ROI images were added to the Cx36 ROI manager, to be overlaid subsequently with the P-Cx36 image, for the measurement of P-Cx36-IR intensity ($I_{P\text{-}Cx36}$) with respect to I_{Cx36} in the same ROI. $I_{P\text{-}Cx36}$ was measured by calculating the summed fluorescence intensity in the P-Cx36 image, in the same area in which the summed fluorescence intensity of Cx36 had been measured. The intensity of plaque labeling was between threshold and saturation of the intensity measurement, and therefore was always within the linear range of measurement. The relative phosphorylation level was estimated by taking a ratio of the intensity of labeling of P-Cx36 to that of Cx36, within the same image region.

Cut-Loading

The cut-loading technique has been used to quantify the extent of tracer coupling among retinal neurons in goldfish and rabbits, under various illumination conditions.[30] It was modified from the procedure described previously by Choi et al.[30] To avoid the influence of diurnal rhythm on HC-HC coupling, animals of different groups were handled in alternating order. In brief, following enucleation and opening of the eye, the retina was isolated and divided into three equal pieces (Fig. 2A). These pieces of retina were laid flat on a filter paper (HAWPO2500, Millipore, MA, USA), photoreceptor-side down, and then submerged in oxygenated Ringer's solution [composition, in mM: 120 NaCl (S7653), 25 $NaHCO_3$ (S9638), 1 NaH_2PO_4 (S6011), 5 KCl (P9333), 10 glucose (G7021), 1 $MgSO_4$ (M22643),0.1 glutamine (G9003), 2 $CaCl_2$ (C8106); Sigma, MD, USA under constant ambient illumination (300 lux or 40 lux) at 36°C in a 5% CO_2/95% O_2 incubator. The retina was immersed in this Ringer's solution during the cutting and loading procedure. The tracer solution (0.5% neurobiotin [SP-1120; Vector Laboratories, Burlingame, CA, USA] + 0.5% rhodamine dextran [341738; Sigma, MD, USA], in Ringer's solution) was prepared immediately before cutting through the retina; rhodamine dextran (> 10,000 MW) does not cross GJs, and thus labels only cells that have been damaged at the cut edge, whereas neurobiotin passes through open GJs, and thus labels cells coupled to the initially exposed ones. A razor blade was dipped in the tracer solution and then used to make a radial cut through the retina and filter paper. The incised retina was incubated for 15 minutes in the incubator, under the same illumination, to allow for loading into the cut cells and diffusion into the network of coupled cells. The retina was then fixed with 4% paraformaldehyde in 0.1 M phosphate buffer (PBS, pH 7.4) for 1 hour at room temperature, washed with 0.1 M PBS overnight at 4°C, incubated overnight at 4°C in 2% streptavidin-Alexa Fluor 488 (S11223; Molecular Probes, Eugene, OR, USA) in 0.1 M PBS + 0.3% Triton X-100, and washed. Finally, the retina was detached from the filter paper, mounted with Vectashield mounting medium (H-1000, Vector Laboratories) on a slide, and cover-slipped.

Images were captured with a laser scanning confocal microscope (Zeiss LSM 880) using a 10x/NA = 0.45 objective lens (image size: 774.44 µm × 774.44 µm; pixel size: 0.83 µm × 0.83 µm). Images including the whole-mounted retina were tiled into one composite image (sizes of tiled images varied from 6.21 mm × 5.44 mm to 7.74 mm × 7.74 mm) – at the same magnification, resolution, and laser intensity settings for every experimental condition. HCs were identified by their distinctive network in the outer INL, and their identity was further confirmed by co-labeling for calbindin (ab75524, Abcam, Cambridge, MA, USA), an HC marker that labels both A- and B-type HCs in guinea pigs (Fig. 1E).[37] A z-stack of images in the area of interest was collapsed into a single image containing all the HC cells in their entirety, and then saved as a 16-bit non-compressed TIF file.

The fluorescence intensity of images of whole-mounted retinas was measured with National Institutes of Health (NIH) ImageJ software. The area of interest was selected to project into the retina from the location of peak fluorescence at the cut border. The width of the area of interest (parallel

Investigative Ophthalmology & Visual Science

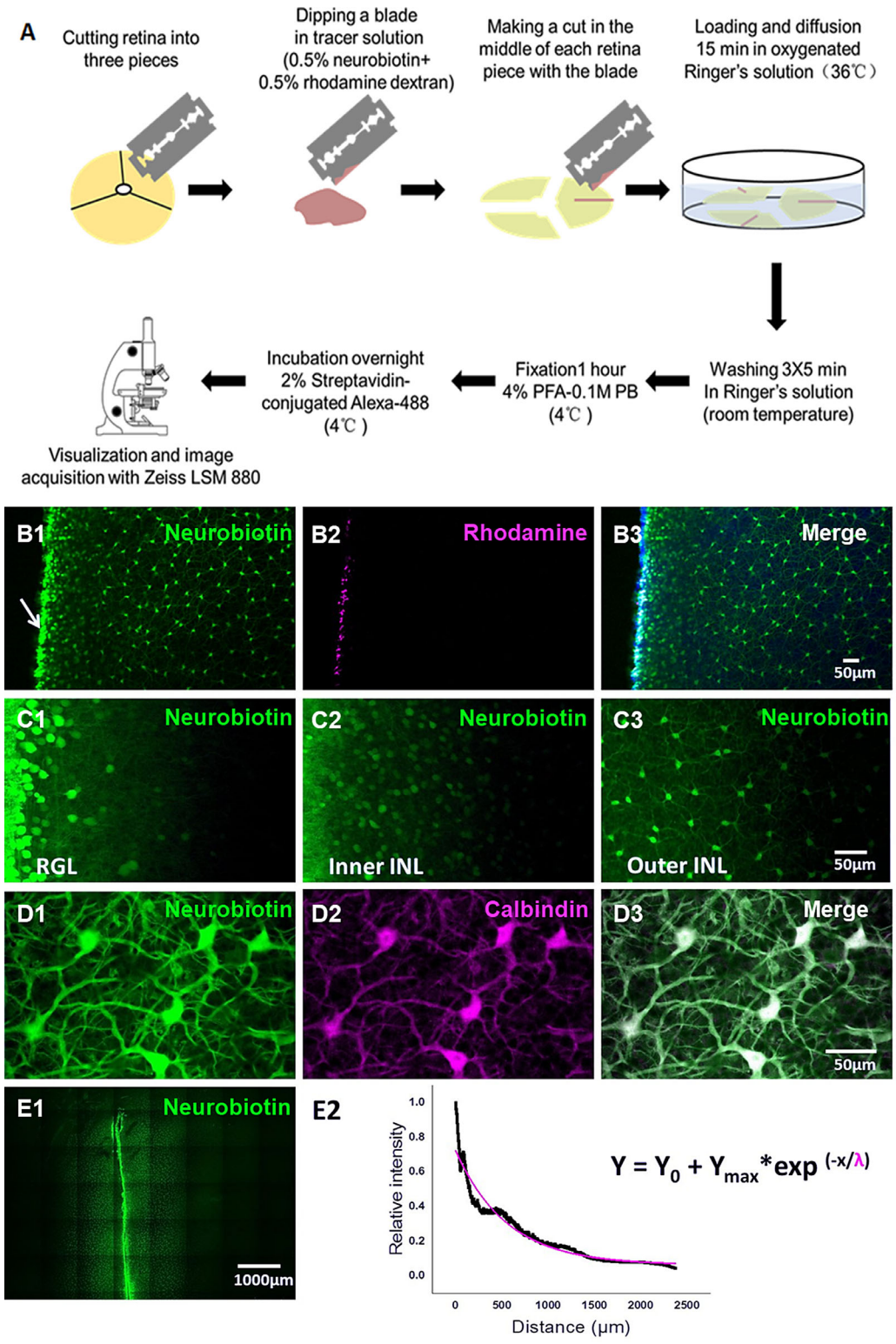

Figure 2. Procedure and analysis of the cut-loading technique. (**A**) Schematic diagram of cut-loading technique. (**B**) A representative example shows fluorescence of a flat-mounted guinea pig retina, following cut-loading with a solution of both neurobiotin (green, **B1**) and rhodamine dextran (magenta, **B2**). Rhodamine dextran labels only damaged cells along the cut, whereas neurobiotin diffuses through GJs between viable cells and can be seen in coupled cells far from the cut. (**C**) The neurobiotin diffuses to different extents in the Retinal Ganglion Cell Layer (RGL, **C1**), inner sublayer of Inner Nuclear Layer (inner INL, **C2**), and outer sublayer of INL (**C3**). In the RGL and inner INL, tracer coupling is limited mainly to a range of less than 300 μm from the cut. In the outer INL, a layer of cells is more extensively coupled (over 1000 μm from the cut). (**D**) The coupled cells in the outer INL (**D1**) are co-labeled for the horizontal cell marker, calbindin (**D2**, **D3**). (**E**) Tracer coupling of horizontal cells is revealed by diffusion of neurobiotin (**E1**); **E2**: Normalized relative fluorescence intensity of the horizontal cell layer as a function of distance from the cut.

Investigative Ophthalmology & Visual Science

to the razor-cut) was 0.9–1.1 mm, and the length depended on the extent of diffusion of the tracer (i.e. the chosen area extended from the cut border to the area without tracer fluorescence). Normalized relative fluorescence intensity, as a function of distance from the cut, was acquired by dividing each raw fluorescence value by the maximum fluorescence value, and then fitted with the EXPONENTIAL DECAY #1 function,[30] which is in the form:

$$Y = Y_0 + Y_{max} * \exp^{(-x/\lambda)}$$

where Y is the relative fluorescence intensity, Y_0 is the background fluorescence, Y_{max} is the maximum relative fluorescence, the exponent (exp) is 2.71828, λ is the space (length) constant, and x is the distance from the cut. The space constant (λ) represents the extent of HC-HC coupling – that is, the value of the space constant is in direct proportion to the extent of coupling.[30]

Statistics

All data are presented as mean ± standard error (M ± SEM). The total intensities of Cx36-IR, P-Cx36-IR plaques, the phosphorylation levels of Cx36-IR plaques ($I_{P\text{-}Cx36/Cx36}$), and the space constants (λ) of tracer diffusion were compared between groups, with an independent *t*-test for two different groups, or one-way analysis of variance (one-way ANOVA) for three different groups, with SPSS (version 15.0). Ocular biometric results of the two eyes of each individual animal were compared using a paired *t*-test. Differences in biometric results between drug-injected groups were compared by 2-way repeated ANOVA. Homogeneity of variance was tested in all groups before analysis with SPSS, and normal distribution was tested with Kolmogorov-Smirnov (K-S) and Shapiro-Wilk (S-W) tests (K-S test: $P > 0.106$; S-W test: $P > 0.105$ for I_{Cx36}, $I_{P\text{-}Cx36}$ and $I_{P\text{-}Cx36}/ I_{Cx36}$ data, K-S test: $P > 0.083$; S-W test: $P > 0.194$ for space constants (i.e. λ). The normality of distribution was confirmed for all data sets, and multiple comparisons between the groups were performed using the Bonferroni correction if homogeneity of variance was satisfied, or using the Dunnett T3 correction if homogeneity of variance was not. Both the intra- and inter-group differences were defined as statistically "significant" if $P < 0.05$, or "highly significant" if $P < 0.01$.

Results

Effects of FD and HD on the Extent of Tracer Coupling Among Horizontal Cells

Space constants (λ) for tracer coupling of HCs were measured in the FD, HD, and NV groups; animals were raised in normal illumination (300 lux) for 2 days, and HC-HC coupling was evaluated on the third day, after light-on for another 1 hour. Space constants were significantly greater in FD eyes than in fellow eyes and normal control eyes (FD-T: 937 ± 126 μm; FD-F: 620 ± 46 μm; NV: 476 ± 65 μm; NV versus FD-T: $P = 0.005$; FD-F versus FD-T: $P = 0.047$; 1-way ANOVA; Fig. 3A); that is, HC-HC coupling in eyes exposed to 300 lux was increased by FD. To exclude effects due to the FD-induced reduction in light level, we also evaluated HC-HC coupling in animals raised in 40 lux (illuminance at the eye, as decreased by FD in 300 lux environment) versus 300 lux. The HC-HC coupling in these animals was also evaluated on the third day after light-on for another 1 hour. λ was significantly less in retinas held at 40 lux (460 ± 43 μm) than in those held at 300 lux (653 ± 84 μm; $P = 0.030$, independent *t*-test; Fig. 3B). To evaluate the effects of HD on HC-HC coupling, we compared HC-HC coupling between animals treated with a −4 D lens versus a 0 D lens. After lens-wear for 2 days, there were no significant differences in λ among the NV, 0 D, and −4 D groups ($P = 0.550$, 1-way ANOVA; Fig. 3C). The greater extent of tracer-coupling in FD eyes was specifically caused by FD, and not by reduced light intensity, because tracer-coupling was less in eyes experiencing unobstructed vision at reduced illuminance and was unaffected by HD.

Effect of HD and FD on the Amount of Cx36 and its Degree of Phosphorylation

In vertical sections of the retina, Cx36 was strongly labeled and characterized by a distinctive punctate appearance in the IPL and OPL (Fig. 4A). In the IPL, the labeled band consisted of tiny, discrete plaques, with a denser distribution in the ON-sublamina than in the OFF-sublamina; in the OPL, the labeled band was thinner, and the plaques were larger and more aggregated. The total fluorescence intensity of Cx36 in both IPL and OPL decreased from 3 weeks of age, when treatments were initiated, to 7 weeks of age, when FD treatment ended (IPL: $P = 0.003$; OPL: $P = 0.004$, independent *t*-test, Table 1: I_{Cx36}, $I_{P\text{-}Cx36}$, and $I_{P\text{-}Cx36}/ I_{Cx36}$).

Wearing a −4 D or 0 D lens for 2 days or 1 week did not alter the total fluorescence intensities in the IPL or OPL, of either Cx36 (at 2 days: IPL: $P = 0.23$, OPL: $P = 0.56$, Fig. 4B; at 1 week: IPL: $P = 0.25$, OPL: $P = 0.67$, Fig. 4E; independent *t*-test) or P-Cx36 (at 2 days: IPL: $P = 0.14$, OPL: $P = 0.59$, Fig. 4C; at 1 week: IPL: $P = 0.28$, OPL: $P = 0.27$, Fig. 4F; independent *t*-test); neither did it alter their fluorescence intensity ratios (at 2 days: IPL: $P = 0.97$, OPL: $P = 0.68$, Fig. 4D; at 1 week: IPL: $P = 0.54$, OPL: $P = 0.28$, Fig. 4G; independent *t*-test), compared to those in the NV group (see Table 1).

FD for 2 days did not result in any significant difference in the total fluorescence intensity of either Cx36 (IPL: $F = 1.107$, $P = 0.352$, OPL: $F = 1.211$, $P = 0.321$; 1-way ANOVA, Fig. 5B) or P-Cx36 (IPL: $F = 1.863$, $P = 0.184$; OPL: $F = 0.845$, $P = 0.446$; 1-way ANOVA, Fig. 5C); there was also no significant difference in the fluorescence intensity ratio for FD eyes, compared to those of the NV-300 lux and NV-40 lux groups (IPL: $F = 0.364$, $P = 0.700$; OPL: $F = 0.161$, $P = 0.852$; 1-way ANOVA; see Fig. 5A,D; Table 1).

FD for 4 weeks reduced the total fluorescence intensity of Cx36 ($P = 0.047$, independent *t*-test, Fig. 6B), P-Cx36 ($P = 0.030$, independent *t*-test, Fig. 6C) and the percentage of phosphorylated Cx36-IR plaques ($P = 0.019$; independent *t*-test, Fig. 6D) in the IPL, compared to equivalent values for the NV group. However, FD for 4 weeks did not significantly affect these descriptive parameters in the OPL (Fig. 6, $P \geq 0.087$ for all parameters tested, independent *t*-test).

Subconjunctival 18-β-GA Injection Induced Myopia in NV Eyes

Before treatment, there were no significant differences between the left and right eyes, in either refraction or ocular axial parameters (ACD, LT, VCD, and AL; $P > 0.05$, paired *t*-test; data not shown).

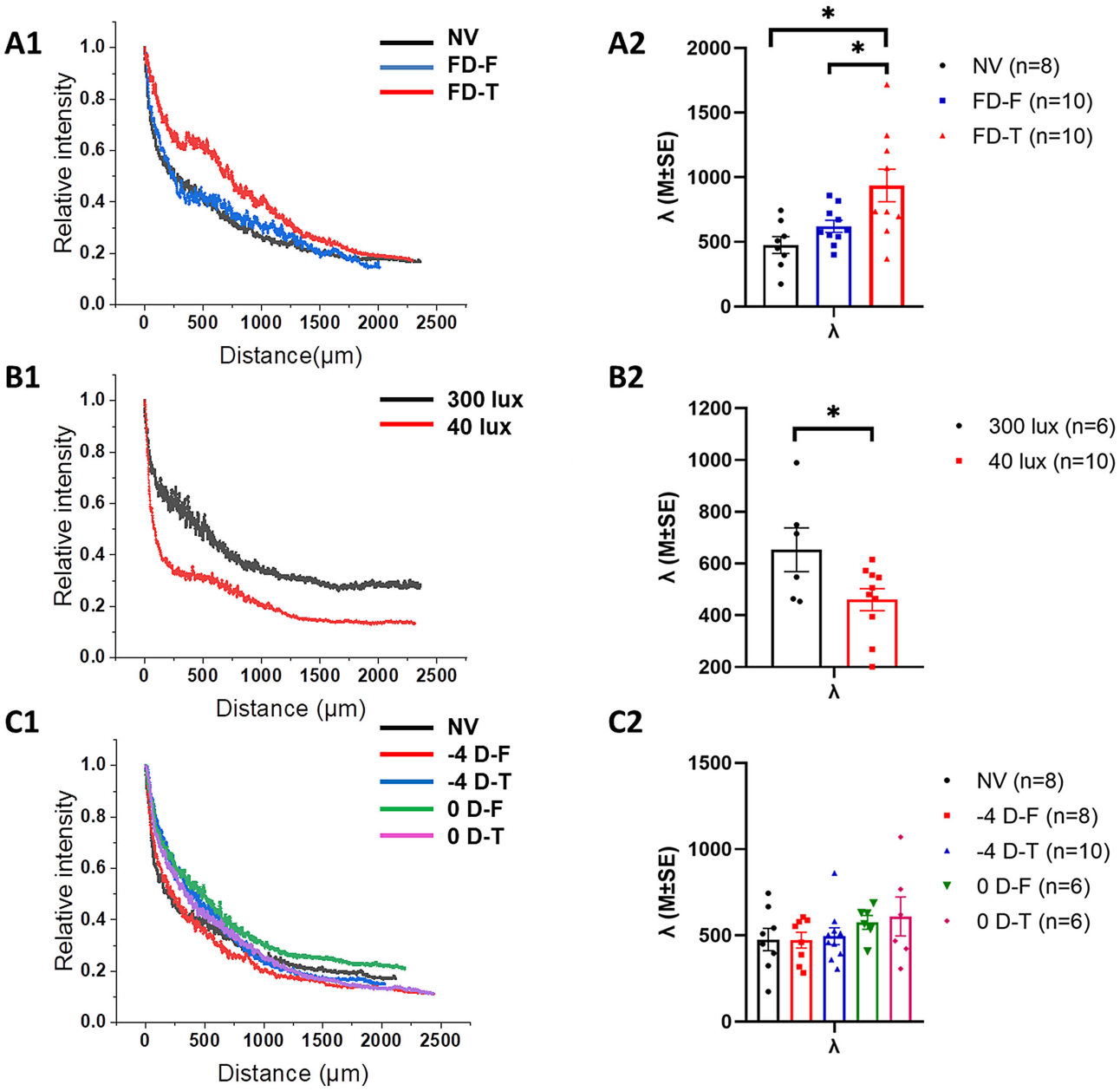

Figure 3. The effects of FD, low illuminance, and HD on horizontal cell tracer coupling after 2 days' treatment. (**A**) FD increased horizontal cell tracer coupling. (**A1**) An example of diffusion curves from animals raised in normal visual environment (NV) and the fellow (FD-F) and treated eyes (FD-T) of the FD animals. (**A2**) The space constants of each group (NV: $n = 8$, FD-F: $n = 10$, and FD-T: $n = 10$). (**B**) Illuminance of 40 lux decreased horizontal cell tracer coupling. (**B1**) Example of diffusion curves from 300 lux and 40 lux groups. (**B2**) Space constants of the two illuminance groups (300 lux: $n = 6$; 40 lux: $n = 10$). (**C**) HD did not affect horizontal cell tracer coupling. (**C1**) Example of diffusion curves from normal vision (NV, $n = 8$), 0 D ($n = 6$), and defocus (−4 D, −4 D-F: $n = 8$; −4 D-T: $n = 11$) groups. (**C2**) The space constants of the −4 D and 0 D groups. *$P < 0.05$.

Daily subconjunctival injection of 18-β-GA shifted refractions towards myopia in the NV environment (Fig. 7A1). The interocular differences in refraction of the NV + V ($n = 12$), NV + 40 μg ($n = 14$), and NV + 120 μg ($n = 13$) groups were −0.51 ± 0.16 D, −1.99 ± 0.31 D and −4.11 ± 0.45 D, respectively, after 2 weeks of 18-β-GA injection, and −0.55 ± 0.16 D, −2.86 ± 0.46 D, and −5.66 ± 0.57 D, respectively, after 4 weeks of injection. There was a significant effect of treatment duration on refraction ($F = 63.364$, $P < 0.001$, 2-way repeated ANOVA), and a significant interaction between duration and dosage ($F = 9.437$, $P < 0.001$, 2-way repeated ANOVA). Eyes in both the NV + 40 μg and NV + 120 μg groups developed higher myopia than those in the NV + V group, and eyes in the NV + 120 μg group also developed higher myopia than those in the NV + 40 μg group (NV + V versus NV + 40 μg: $P = 0.006$; NV + V versus NV + 120 μg: $P < 0.001$; NV + 40 μg versus NV + 120 μg: $P = 0.005$, post hoc test; Fig. 7A1).

VCD and AL in the 18-β-GA injection groups increased in parallel with the increases in refractive error. The interocu-

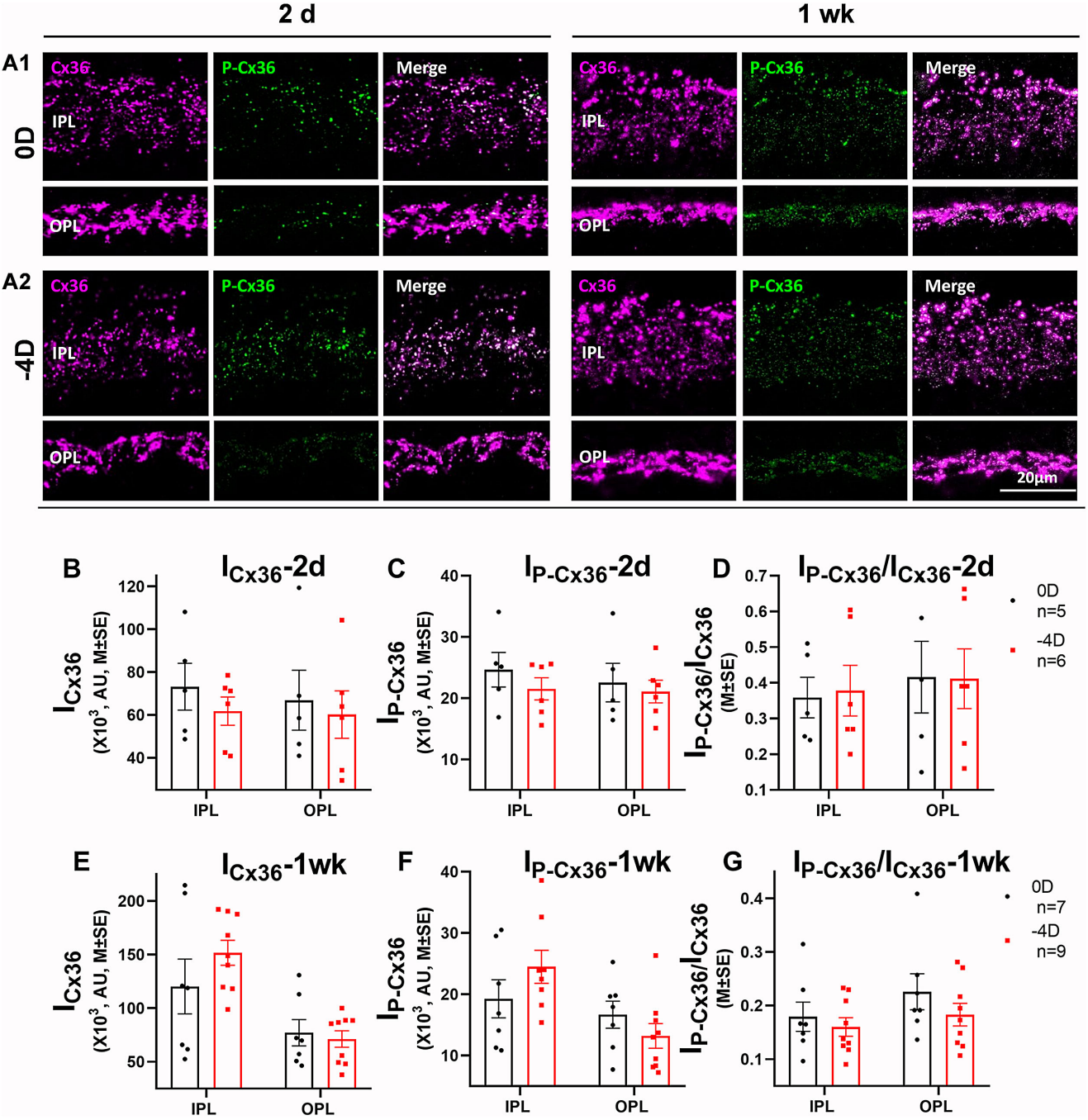

Figure 4. Effects of HD on the fluorescence intensities of retinal Cx36 and P-Cx36 (M ± SE). (**A**) Fluorescence images of vertical sections of guinea pig retina in 0 D and −4 D groups for 2 days and 1 week. (**A1**) 0 D; (**A2**) −4 D; Left panel: HD for 2 days; Right panel: HD for 1 week. (**B**) Total fluorescence intensity of Cx36 in IPL and OPL after HD 2 days. (**C**) Total fluorescence intensity of P-Cx36 in IPL and OPL after HD 2 days. (**D**) Fluorescence intensity ratios (P-Cx36/Cx36) in IPL and OPL after HD 2 days. (**E**) Total fluorescence intensity of Cx36 in IPL and OPL after HD 1 week. (**F**) Total fluorescence intensity of P-Cx36 in IPL and OPL after HD 1 week. (**G**) Fluorescence intensity ratios (P-Cx36/Cx36) in IPL and OPL after HD 1 week. Wearing −4 D or 0 D lens for 2 days and 1 week did not significantly affect either the fluorescence intensity of Cx36 or P-Cx36, or the phosphorylation level of Cx36 (P-Cx36:Cx36), in either IPL or OPL. AU units represent relative fluorescence intensity.

lar differences in VCD of the NV + V, NV + 40 μg, and NV + 120 μg groups were 0.01 ± 0.01 mm, 0.03 ± 0.01 mm, and 0.04 ± 0.01 mm, respectively, after 2 weeks of 18-β-GA injection, and 0.02 ± 0.01 mm, 0.01 ± 0.01 mm, and 0.03 ± 0.01 mm, respectively, after 4 weeks of injection. There was a significant effect of treatment duration on VCD ($F = 202.501$, $P < 0.001$, 2-way repeated ANOVA), and a significant interaction between duration and dosage ($F = 2.706$, $P = 0.038$, 2-way repeated ANOVA). Only eyes in the NV + 40 μg group developed longer VCD than those in the NV + V group; but there was no significant difference between either the NV + 120 μg and NV + V eyes, or between the

Investigative Ophthalmology & Visual Science

Table 1. The Amounts and Phosphorylation-Levels of Cx36 after FD and 18-β-GA Injection

		Location	Group	Intensity of Cx36 ($\times 10^3$ AU)	Intensity of P-Cx36 ($\times 10^3$ AU)	Ratio of Intensity (P-Cx36/Cx36)
FD	**2 days**	IPL	NV-300 lux ($n = 7$)	83.22 ± 11.36	28.08 ± 2.69	0.38 ± 0.06
			NV-40 lux ($n = 7$)	64.29 ± 12.61	21.49 ± 5.68	0.34 ± 0.06
			FD-T ($n = 7$)	95.06 ± 19.09	34.50 ± 5.34	0.40 ± 0.05
		OPL	NV-300 lux ($n = 7$)	52.68 ± 3.97	16.26 ± 3.92	0.33 ± 0.09
			NV-40 lux ($n = 7$)	62.53 ± 11.84	19.18 ± 3.92	0.32 ± 0.07
			FD-T ($n = 7$)	72.12 ± 8.85	23.10 ± 3.33	0.38 ± 0.08
	4 wks	IPL	NV ($n = 9$)	9.19 ± 0.91	4.32 ± 0.71	0.46 ± 0.06
			FD-T ($n = 6$)	6.03 ± 0.11*	1.45 ± 0.39*	0.25 ± 0.05*
		OPL	NV ($n = 9$)	10.04 ± 1.8	4.37 ± 0.78	0.45 ± 0.04
			FD-T ($n = 6$)	6.34 ± 1.05	2.64 ± 0.75	0.36 ± 0.07
HD	**2 days**	IPL	−4 D ($n = 6$)	61.80 ± 6.60	21.51 ± 1.81	0.38 ± 0.07
			0 D ($n = 5$)	78.37 ± 12.46	26.59 ± 2.67	0.37 ± 0.07
		OPL	−4 D ($n = 6$)	60.17 ± 11.08	21.07 ± 1.84	0.41 ± 0.08
			0 D ($n = 5$)	71.97 ± 16.83	23.26 ± 3.96	0.42 ± 0.13
	1 wks	IPL	−4 D ($n = 9$)	151.68 ± 11.66	23.68 ± 2.51	0.16 ± 0.02
			0 D ($n = 7$)	120.31 ± 25.57	19.27 ± 3.10	0.18 ± 0.03
		OPL	−4 D ($n = 9$)	71.24 ± 7.68	13.21 ± 2.01	0.18 ± 0.02
			0 D ($n = 7$)	77.25 ± 12.25	16.67 ± 2.21	0.23 ± 0.03
18-β-GA	**4 wks**	IPL	NV ($n = 6$)	11.33 ± 0.77	6.81 ± 0.92	0.60 ± 0.06
			NV + V ($n = 6$)	14.48 ± 0.18	7.87 ± 0.89	0.55 ± 0.02
			NV + 18-β-GA ($n = 11$)	9.47 ± 0.76#	3.35 ± 0.39#,$	0.38 ± 0.03#,$
		OPL	NV ($n = 6$)	17.90 ± 1.05	10.00 ± 0.80	0.57 ± 0.06
			NV + V ($n = 6$)	20.19 ± 1.98	10.42 ± 1.06	0.53 ± 0.04
			NV + 18-β-GA ($n = 11$)	10.81 ± 1.52#	4.38 ± 0.68#,$	0.42 ± 0.07

* $P < 0.05$, independent t-test, FD-T versus NV.
# $P < 0.05$, 1-way ANOVA, NV + 18-β-GA versus NV + V.
$ $P < 0.05$, 1-way ANOVA, NV + 18-β-GA versus NV.

NV + 40 µg and NV + 120 µg groups, in their interocular differences in VCD (VCD: NV + V versus NV + 40 µg: $P = 0.038$; NV + V versus NV + 120 µg: $P = 0.149$; NV + 40 µg versus NV + 120 µg: $P = 1.000$, post hoc test; Fig. 7A2). AL in the 18-β-GA injection groups increased in parallel with the myopic shifts in refractive error. The interocular differences in AL of the NV + V, NV + 40 µg, and NV + 120 µg groups were 0.01 ± 0.01 mm, 0.05 ± 0.01 mm, and 0.07 ± 0.01 mm, respectively, after 2 weeks of 18-β-GA injection, and 0.01 ± 0.01 mm, 0.05 ± 0.01 mm, and 0.05 ± 0.01 mm, respectively, after 4 weeks of injection. There was a significant effect of treatment duration on AL ($F = 15.757$, $P < 0.001$, 2-way repeated ANOVA), and a significant interaction between duration and dosage ($F = 6.537$, $P = 0.004$, 2-way repeated ANOVA). Eyes in both the NV + 40 µg and NV + 120 µg groups developed greater axial lengths than those in the NV + V group, but there were no significant differences in AL between the NV + 40 µg and NV + 120 µg groups (AL: NV + V versus NV + 40 µg: $P = 0.035$; NV + V versus NV + 120 µg: $P = 0.005$; NV + 40 µg versus NV + 120 µg: $P = 1.000$; post hoc test; Fig. 7A3). Injection of 18-β-GA had no statistically significant effects on ACD or LD (Table 2: Ocular biometry).

Subconjunctival Injection of GJ Blocker 18-β-GA Made FD Eyes Slightly More Myopic

Before treatment, there were no significant differences between the left and right eyes, either in refraction or in ocular axial parameters (ACD, LT, VCD, and AL; $P > 0.05$, paired t-test).

Daily subconjunctival delivery of 18-β-GA to FD eyes shifted the refraction towards myopia (Fig. 7B1). The interocular differences in refraction of the FD + V ($n = 17$), FD + 40 µg ($n = 18$), and FD + 120 µg ($n = 18$) groups were −5.15 ± 0.41 D, −6.44 ± 0.57 D, and −6.11 ± 0.65 D, respectively, after 2 weeks of 18-β-GA injection, and −8.94 ± 0.49 D, −10.71 ± 0.56 D, and −11.25 ± 0.62 D, respectively, after 4 weeks of injection. There was a significant effect of duration ($F = 432.224$, $P < 0.001$, 2-way repeated ANOVA) and a significant interaction between duration and dosage in refraction of the FD groups ($F = 3.397$, $P < 0.012$, 2-way repeated ANOVA). Only eyes in the FD + 120 µg group developed higher myopia than those in the FD + V group, and there were no significant differences between FD + 40 µg and FD + V groups or between the FD + 40 µg and FD + 120 µg groups (FD + V versus FD + 40 µg: $P = 0.051$; FD + V versus FD + 120 µg: $P = 0.027$; FD + 40 µg versus FD + 120 µg; $P = 1.000$, post hoc test; Fig. 7B1).

In contrast to the refractive error differences described above, 18-β-GA injection did not increase VCD or AL in the FD groups. There was a significant effect of treatment duration ($F = 210.152$, $P < 0.001$, 2-way repeated ANOVA), and a significant interaction between duration and dosage, for VCD in the FD eyes ($F = 2.712$, $P = 0.035$, 2-way repeated ANOVA), but there were no significant differences in VCD between groups receiving different doses (VCD: FD + V versus FD + 40 µg: $P = 1.000$; FD + V versus FD + 120 µg: $P = 1.000$; FD + 40 µg versus FD + 120 µg; $P = 0.753$, post hoc test; Fig. 7B2). There was a significant effect of treatment duration ($F = 259.034$, $P < 0.001$, 2-way repeated ANOVA), but no significant interaction between duration and dosage, for AL of the FD groups ($F = 0.909$, $P = 0.462$,

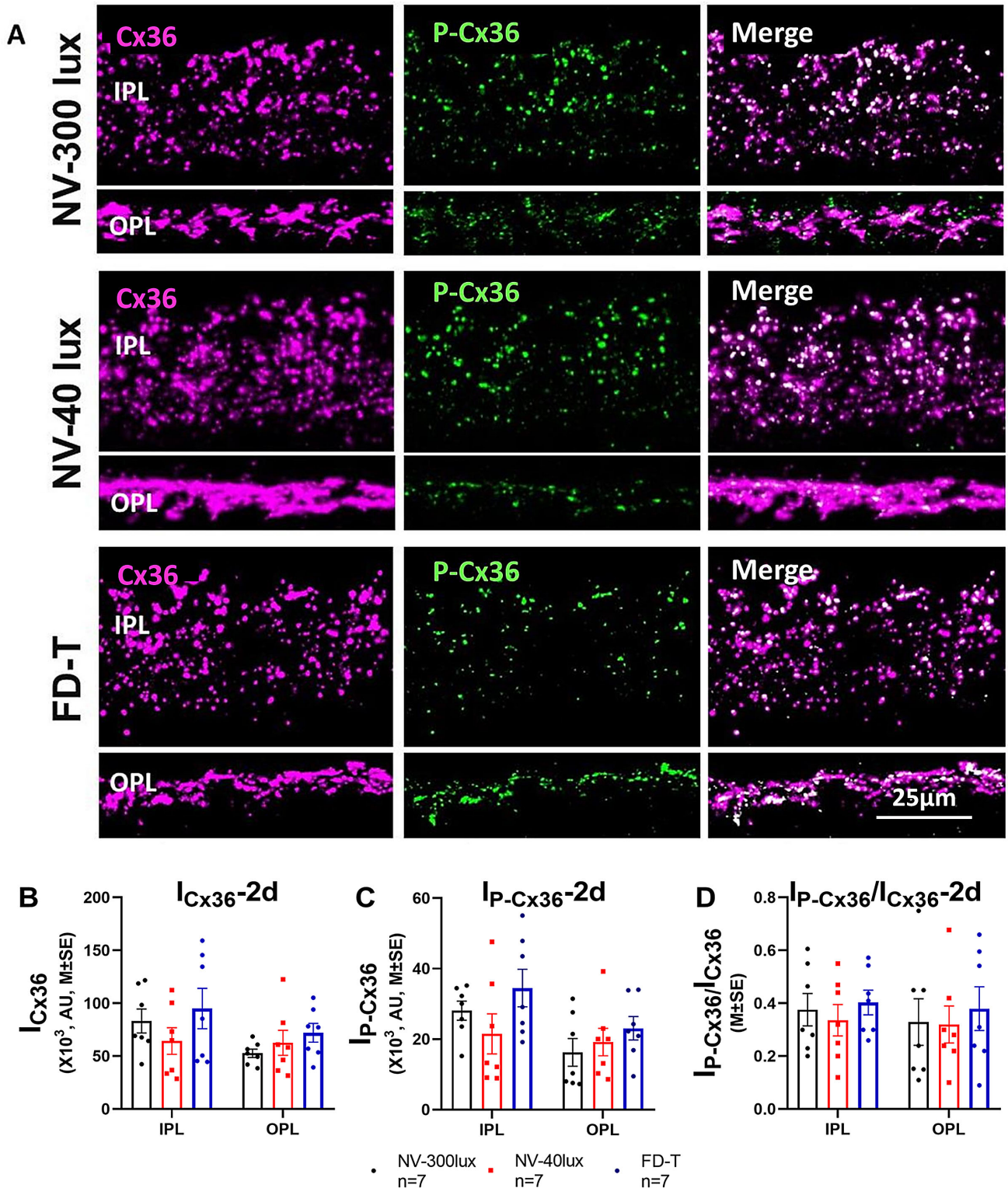

Figure 5. FD for 2 days: The effects of FD and low illuminance on the fluorescence intensity of retinal Cx36 and P-Cx36 (M ± SE). (**A**) Fluorescence images of vertical sections of guinea pig retina of the FD-T ($n = 7$), NV-300 lux ($n = 7$), NV-40 lux ($n = 7$) groups. **A1**: Cx36; **A2**: P-Cx36; **A3**: Merged. (**B**) Total fluorescence intensity of Cx36 in IPL and OPL. (**C**) Total fluorescence intensity of P-Cx36 in IPL and OPL. (**D**) Fluorescence intensity ratios (P-Cx36/Cx36) in IPL and OPL. FD for 2 days did not significantly affect the total fluorescence intensities of Cx36 or P-Cx36 nor the phosphorylation levels of Cx36 (P-Cx36/Cx36), in either IPL or OPL, at either illuminance. AU units represent relative fluorescence intensity.

Investigative Ophthalmology & Visual Science

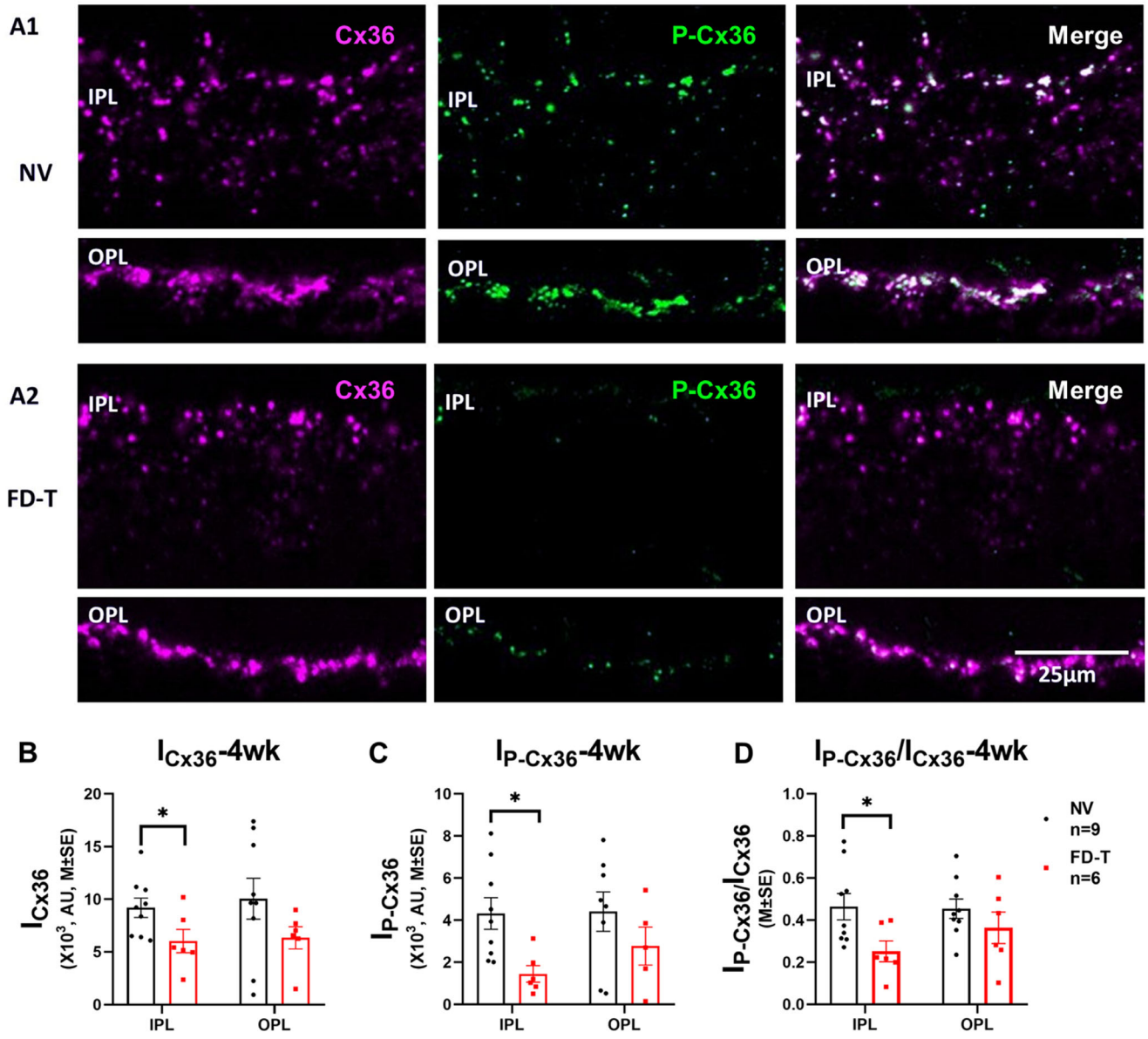

Figure 6. FD for 4 weeks reduced the levels of Cx36 and its phosphorylation in IPL and OPL (M ± SE). (**A**) Immunofluorescence of Cx36 and P-Cx36 in IPL and OPL. **A1: NV** (n = 9); **A2: FD-T** (n = 6). Magenta: Cx36; Green: P-Cx36; White: Merge. (**B**) FD decreased the total intensity of Cx36-IR plaques in IPL. (**C**) FD decreased the total intensity of P-Cx36-IR plaques in IPL. (**D**) FD decreased the phosphorylation level of Cx36 ($I_{P\text{-}Cx36}$/ I_{Cx36}) in IPL. *P < 0.05, independent t-test. AU units represent relative fluorescence intensity.

2-way repeated ANOVA; Fig. 7B3). Thus, injection of 18-β-GA had no statistically significant effects on ACD or LD (see Table 2).

Effect of 18-β-GA on Gap Junction Coupling Among Horizontal Cells

Injection of 18-β-GA, 120 μg/100 μl daily for 2 days reduced tracer diffusion in the HC network of injection groups (F = 4.851, P = 0.019, 1-way ANOVA). There was no significant difference in λ between the NV (n = 8) and NV + V (n = 7) groups (NV versus NV + V: 476 ± 64 vs. 729 ± 88; P = 0.083, post hoc test, Fig. 8A). In contrast, λ was significantly lower in the NV + 18-β-GA (n = 8) than in NV + V groups (NV + V versus NV + 18-β-GA: 729 ± 88 vs. 413 ± 71; P = 0.023, post hoc test, see Fig. 8A).

Effect of 18-β-GA on Amount and Phosphorylation of Retinal Cx36

All the data satisfied the condition of homogeneity of variance (P > 0.056), except for the fluorescence intensity of P-Cx36 (P = 0.041) and the fluorescence intensity ratio of Cx36 and P-Cx36 (P = 0.037) in the IPL. There were no significant differences between the measured parameters (I_{Cx36}, $I_{P\text{-}Cx36}$, and $I_{P\text{-}Cx36}/I_{Cx36}$) in the NV + V and NV groups,

Investigative Ophthalmology & Visual Science

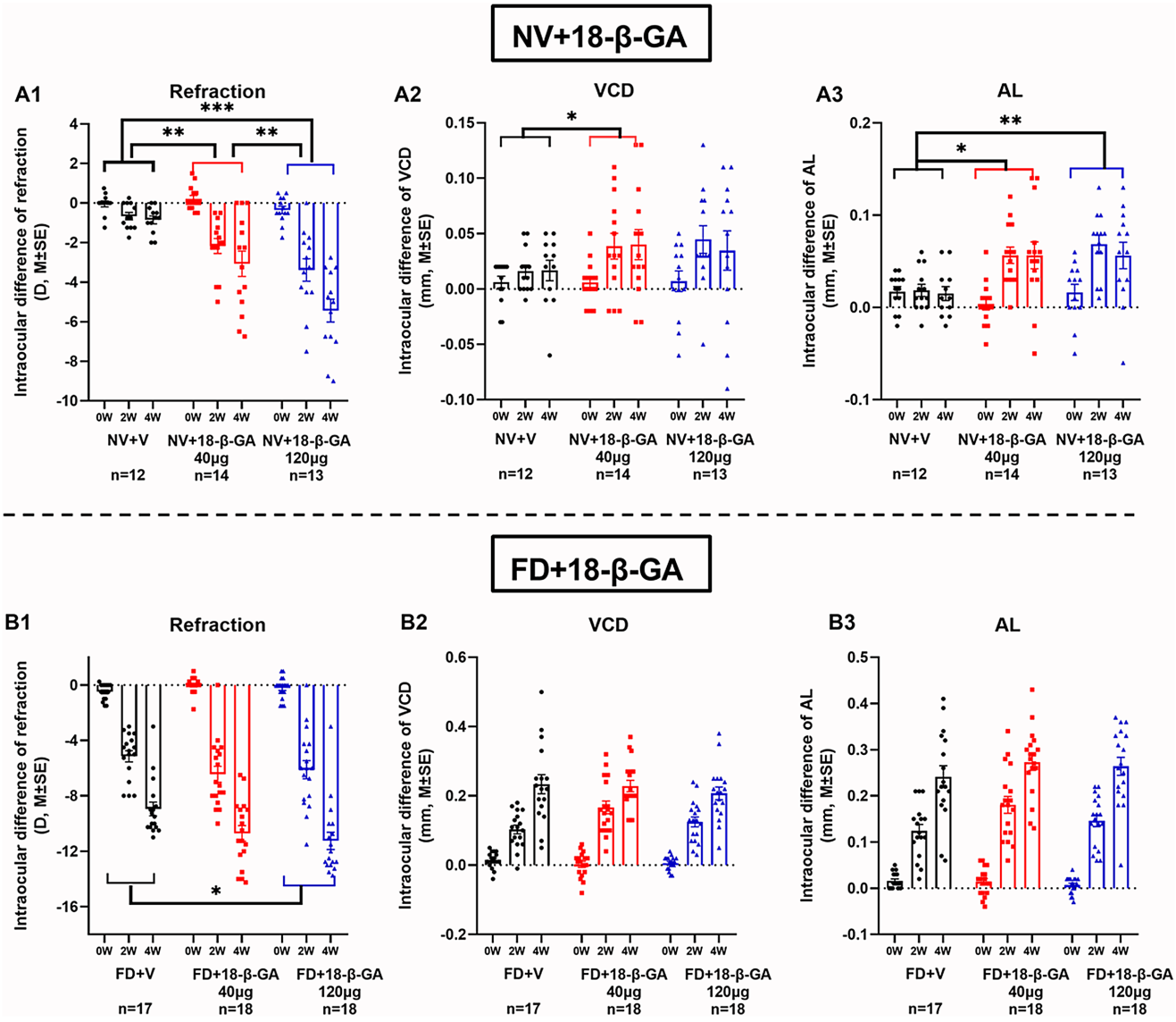

Figure 7. Subconjunctival injection of 18-β-GA enhanced ocular elongation and myopia development, in normal vision (NV) and form-deprivation (FD) conditions (M ± SE). (**A**) Interocular differences of refraction (**A1**), vitreous chamber depth (VCD) (**A2**), and axial length (AL) (**A3**), in NV. (**B**) Interocular differences of refraction (**B1**), vitreous chamber depth (VCD) (**B2**) and axial length (AL) (**B3**), in FD. Injection of 18-β-GA induced myopia development in both NV (**A1**) and FD (**B1**). VCD and AL were consistently increased in NV (**A2**, **A3**), but not obviously in FD (**B2**, **B3**). * $P < 0.05$; ** $P < 0.01$; *** $P < 0.001$, 2-way repeated ANOVA, Bonferroni correction, post hoc test.

in either the IPL ($P > 0.214$) or OPL ($P > 0.742$, 1-way ANOVA; Fig. 8C, 8D, 8E). In the IPL, injection of 18-β-GA (120 μg/100 μL) for 4 weeks decreased the overall fluorescence intensities of Cx36 (I_{Cx36}, F = 5.681, $P = 0.009$, 1-way ANOVA, see Fig. 8C), P-Cx36 ($I_{P\text{-}Cx36}$, F = 11.173, $P < 0.001$, 1-way ANOVA, see Fig. 8D) and decreased the phosphorylation of Cx36-IR plaques ($I_{P\text{-}Cx36}/I_{Cx36}$; F = 10.877, $P = 0.001$, 1-way ANOVA; see Fig. 8E). Injection of 18-β-GA reduced I_{Cx36} in the IPL in the NV eyes, compared to the NV + V eyes, but not compared to the NV eyes (NV: 11.33 ± 0.77, NV + V: 14.48 ± 0.18, NV + 18-β-GA: 9.47 ± 0.76; NV + V versus NV + 18-β-GA: $P = 0.009$, NV versus NV + 18-β-GA: $P = 0.818$, post hoc test). Injection of 18-β-GA also reduced $I_{P\text{-}cx36}$ (NV: 6.81 ± 0.92, NV + V: 7.87 ± 0.89, NV + 18-β-GA: 3.35 ± 0.39; NV + V versus NV + 18-β-GA: $P = 0.027$, NV versus NV + 18-β-GA: $P = 0.016$, post hoc test) and $I_{P\text{-}Cx36}/I_{Cx36}$ (NV: 0.60 ± 0.06, NV + V: 0.55 ± 0.02, NV + 18-β-GA: 0.38 ± 0.03; NV + V versus NV + 18-β-GA: $P = 0.027$, NV versus NV + 18-β-GA: $P = 0.03$, post hoc test) in the IPL when compared to the NV + V and NV groups. In the OPL, injection of 18-β-GA reduced I_{Cx36} (F = 3.716, $P = 0.042$, 1-way ANOVA; see Fig. 8C), but there was no significant difference among any pair of the NV, NV + V, and NV + 18-β-GA groups. Injection of 18-β-GA also reduced $I_{P\text{-}cx36}$ in the OPL (NV: 10.00 ± 0.80, NV + V: 10.42 ± 1.06, NV + 18-β-GA: 4.38 ± 0.68; F = 8.297, $P = 0.02$, 1-way ANOVA; NV + V versus NV + 18-β-GA: $P = 0.005$, NV versus NV + 18-β-GA: p = 0.017; post hoc test; See Fig. 8D). The $I_{P\text{-}Cx36}/I_{Cx36}$ ratio in OPL was not altered by injection of 18-β-GA (F = 1.781, $P = 0.194$, 1-way ANOVA; see Fig. 8E, Table 2).

Table 2. Ocular Biometrics of Guinea Pigs Before and After 18-β-GA Injection in Normal Visual Environment or After Form Deprivation

	Group	Eye	Refraction (D)	ACD (mm)	LT (mm)	VCD (mm)	AL (mm)
2W	**NV + V**	**OD**	5.01 ± 0.34	1.12 ± 0.01	3.89 ± 0.02	3.19 ± 0.02	8.21 ± 0.04
	$n = 12$	**OS**	5.53 ± 0.28	1.13 ± 0.02	3.88 ± 0.02	3.18 ± 0.02	8.20 ± 0.03
		OD-OS	−0.51 ± 0.16	−0.01 ± 0.01	0.01 ± 0.01	0.01 ± 0.01	0.01 ± 0.01
	NV + 18-β-GA	**OD**	3.43 ± 0.40	1.14 ± 0.01	3.92 ± 0.03	3.23 ± 0.02	8.26 ± 0.03
	40 μg	**OS**	5.61 ± 0.20	1.14 ± 0.01	3.90 ± 0.02	3.19 ± 0.02	8.21 ± 0.03
	$n = 14$	**OD-OS**	−2.19 ± 0.31	0.00 ± 0.01	0.02 ± 0.01	0.03 ± 0.01	0.05 ± 0.01
	NV + 18-β-GA	**OD**	2.07 ± 0.53	1.12 ± 0.02	3.92 ± 0.03	3.21 ± 0.02	8.27 ± 0.03
	120 μg	**OS**	6.18 ± 0.30	1.12 ± 0.02	3.90 ± 0.02	3.19 ± 0.02	8.20 ± 0.03
	$n = 13$	**OD-OS**	−4.11 ± 0.45	0.00 ± 0.01	0.02 ± 0.02	0.04 ± 0.01	0.07 ± 0.01
	FD + V	**OD**	0.65 ± 0.45	1.12 ± 0.01	3.89 ± 0.03	3.30 ± 0.02	8.32 ± 0.04
	$n = 17$	**OS**	5.79 ± 0.22	1.14 ± 0.01	3.86 ± 0.03	3.20 ± 0.02	8.19 ± 0.03
		OD-OS	−5.15 ± 0.41	−0.02 ± 0.01	0.03 ± 0.01	0.10 ± 0.01	0.12 ± 0.01
	FD + 18-β-GA	**OD**	−0.49 ± 0.43	1.12 ± 0.01	3.91 ± 0.02	3.35 ± 0.02	8.39 ± 0.03
	40 μg	**OS**	5.96 ± 0.38	1.11 ± 0.01	3.91 ± 0.02	3.19 ± 0.03	8.21 ± 0.02
	$n = 18$	**OD-OS**	−6.44 ± 0.57	0.01 ± 0.01	0.00 ± 0.01	0.17 ± 0.02	0.18 ± 0.02
	FD + 18-β-GA	**OD**	−0.21 ± 0.76	1.13 ± 0.02	3.89 ± 0.02	3.31 ± 0.02	8.34 ± 0.03
	120 μg	**OS**	5.90 ± 0.34	1.16 ± 0.01	3.86 ± 0.02	3.18 ± 0.02	8.20 ± 0.03
	$n = 18$	**OD-OS**	−6.11 ± 0.65	-0.03 ± 0.01	0.03 ± 0.01	0.13 ± 0.01	0.15 ± 0.01
4W	**NV + V**	**OD**	5.20 ± 0.24	1.14 ± 0.01	4.02 ± 0.03	3.22 ± 0.02	8.35 ± 0.03
	$n = 12$	**OS**	5.75 ± 0.27	1.15 ± 0.01	3.99 ± 0.02	3.21 ± 0.02	8.35 ± 0.02
		OD-OS	−0.55 ± 0.26	-0.01 ± 0.01	0.03 ± 0.02	0.02 ± 0.01	0.01 ± 0.01
	NV + 18-β-GA	**OD**	2.35 ± 0.45	1.14 ± 0.02	4.08 ± 0.02	3.26 ± 0.02	8.45 ± 0.03
	40 μg	**OS**	5.28 ± 0.22	1.16 ± 0.02	4.05 ± 0.02	3.22 ± 0.02	8.40 ± 0.03
	$n = 14$	**OD-OS**	−2.86 ± 0.46**	−0.02 ± 0.01	0.04 ± 0.01	0.04 ± 0.01*	0.05 ± 0.01*
	NV + 18-β-GA	**OD**	−0.27 ± 0.54	1.13 ± 0.01	4.06 ± 0.03	3.23 ± 0.02	8.42 ± 0.03
	120 μg	**OS**	5.43 ± 0.34	1.14 ± 0.02	4.03 ± 0.03	3.20 ± 0.02	8.38 ± 0.03
	$n = 13$	**OD-OS**	−5.46 ± 0.57***,#	0.00 ± 0.01	0.03 ± 0.01	0.03 ± 0.02	0.05 ± 0.01**
	FD + V	**OD**	−3.07 ± 0.53	1.15 ± 0.02	4.03 ± 0.02	3.43 ± 0.02	8.60 ± 0.03
	$n = 17$	**OS**	5.87 ± 0.22	1.17 ± 0.02	3.99 ± 0.02	3.20 ± 0.02	8.36 ± 0.03
		OD-OS	−8.94 ± 0.49	0.02 ± 0.01	0.04 ± 0.01	0.23 ± 0.02	0.24 ± 0.02
	FD + 18-β-GA	**OD**	−4.25 ± 0.49	1.12 ± 0.01	4.08 ± 0.02	3.44 ± 0.03	8.65 ± 0.03
	40 μg	**OS**	6.46 ± 0.25	1.13 ± 0.01	4.03 ± 0.02	3.20 ± 0.02	8.38 ± 0.03
	$n = 18$	**OD-OS**	−10.71 ± 0.56	−0.01 ± 0.01	0.05 ± 0.01	0.23 ± 0.02	0.27 ± 0.02
	FD + 18-β-GA	**OD**	−5.60 ± 0.44	1.16 ± 0.02	4.07 ± 0.02	3.41 ± 0.02	8.64 ± 0.02
	120 μg	**OS**	5.65 ± 0.32	1.16 ± 0.02	4.02 ± 0.02	3.20 ± 0.02	8.38 ± 0.03
	$n = 18$	**OD-OS**	−11.25 ± 0.62*	0.00 ± 0.01	0.05 ± 0.02	0.21 ± 0.02	0.26 ± 0.02

*$P < 0.05$,
**$P < 0.01$,
***$P < 0.001$, compared to the vehicle groups.
#$P < 0.05$, compared to the 40 μg groups.

Discussion

The Role of Cx36 in Myopia Development

This study in pigmented guinea pigs found that 4 weeks of treatment with FD or NV + 18-β-GA induced myopia, while simultaneously reducing the amount of Cx36 and its level of phosphorylation in the IPL (see Figs. 6, 7, 8). This suggests that Cx36-mediated cell-cell coupling in the guinea pig retina is involved in the cascade driving FDM development. In animals treated with both 18-β-GA and FD, the amplitude of myopic shifts was smaller than the linear summation of amplitudes in animals treated with 18-β-GA or FD alone (see Fig. 7). These findings indicate that in animals treated with both 18-β-GA and FD, a portion of the response to FD is mediated by effects on GJ coupling; therefore, Cx36 might be the target of both FD (which affects GJs and other targets) and 18-β-GA (which affects mainly GJs). It is also worth noting that the effects of 18-β-GA injection on VCD and AL were not in parallel with the changes of refraction. There were no significant differences in VCD and AL between the FD + 18-β-GA and FD + V groups, after 2 weeks or 4 weeks of treatment, although 18-β-GA made the FD groups slightly more myopic than did FD alone. These results indicate that 18-β-GA may also affect other ocular refractive components besides VCD and AL – because gap junctions are present not only in multiple neural circuits in the retina, but also in non-retinal ocular tissues (lens,[38] retinal pigment epithelium,[39] choroid,[40] and sclera[41]) that are accessible to the subconjunctivally injected drug. FD induced a higher degree of myopia than did 18-β-GA injection, suggesting that the coupling mediated by retinal GJs contributes only partially to FDM development, or that the roles of GJs on ocular growth and refraction may be complementary and therefore counteract one another. In contrast, HD – which also induces myopia – did not affect the amount of retinal Cx36 or its level of phosphorylation (see Fig. 4). These results indicate that GJs containing Cx36, especially those in the IPL, might play a functional role in FDM – but not in LIM.

We have found here that the distribution of Cx36-containing plaques in the IPL in the guinea pig retina is similar to that reported previously in the human retina, with a much higher number of plaques in the ON-sublamina than

Investigative Ophthalmology & Visual Science

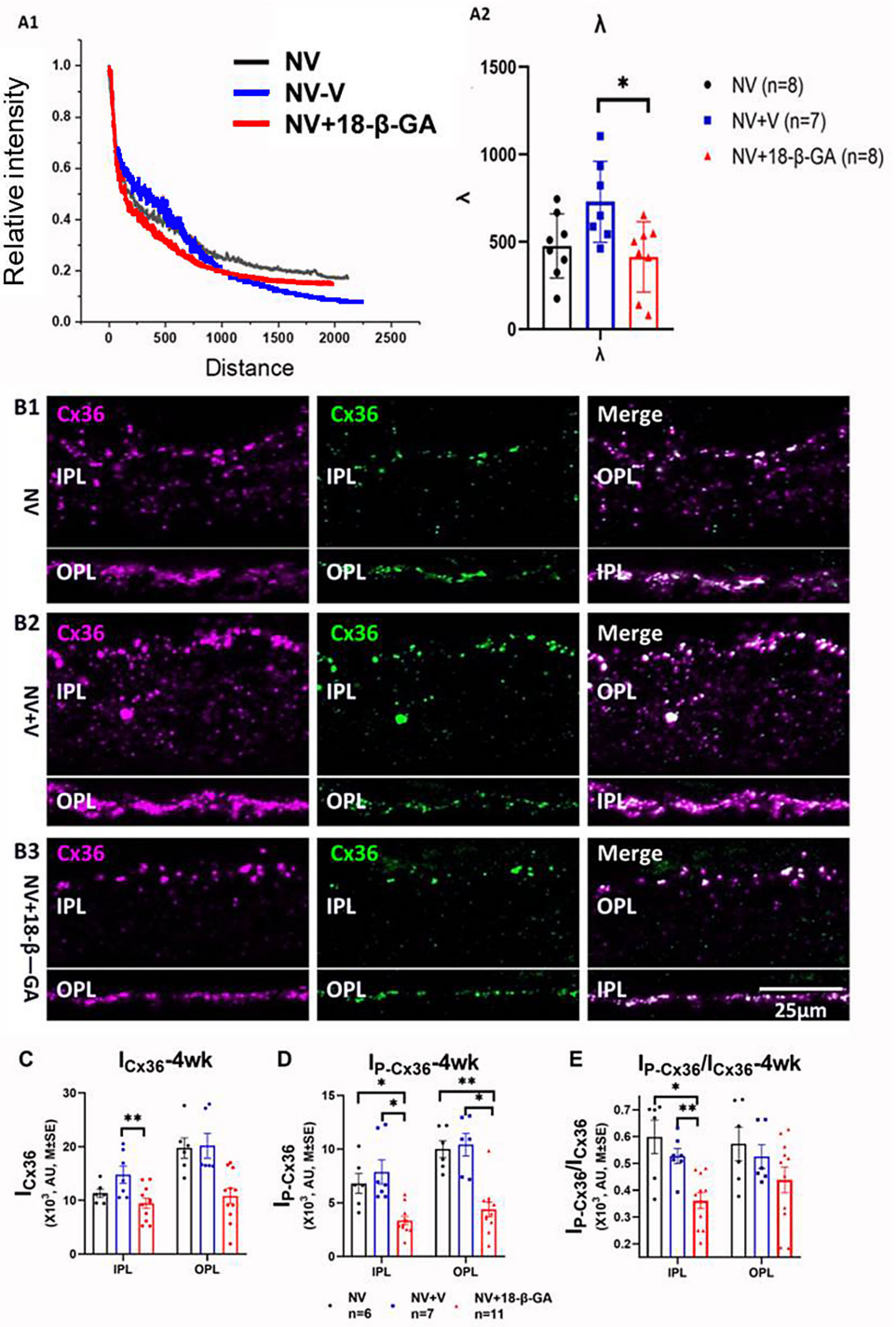

Figure 8. Effects of 18-β-GA on horizontal cell tracer coupling (at day 2), Cx36 protein content, and Cx36 phosphorylation (at week 4). Injection of 18-β-GA decreased horizontal cell tracer coupling (M $\pm$ SE) (**A**). (**B**) Immunofluorescence of Cx36 and P-Cx36 in the IPL and OPL of retinas treated by 18-β-GA-injection. (**B1**) NV ($n = 13$); (**B2**)NV + V ($n = 7$); (**B3**): NV + 18-β-GA ($n = 11$). Magenta: Cx36; Green: P-Cx36; White: Merged Cx36 + P-Cx36. Injection of 18-β-GA decreased the levels of Cx36 (**C**), P-Cx36 (**D**), and Cx36 phosphorylation (P-Cx36:Cx36) in IPL (**E**), in comparison to NV + V controls (M $\pm$ SE). * $P < 0.05$; ** $P < 0.01$; *** $P < 0.001$, 1-way ANOVA. AU units represent relative fluorescence intensity.

in the OFF-sublamina.[29] The I_{Cx36} of the -4 D group was significantly higher at week 1 than that at day 2, possibly because we used a new lot of anti-Cx36 antibody for this part of our study. Cx36-containing GJs in the IPL are critically involved in the primary rod pathway,[17,42] whereas those in the OPL are involved in the secondary rod pathway in guinea pigs.[43] Phosphorylation of Cx36 increases coupling via GJs containing Cx36.[36,44] Both FD and 18-β-GA injections induced myopia, with consistently parallel effects on the amount and phosphorylation of Cx36 in the IPL,

suggesting that Cx36-containing GJs might affect emmetropization via the rod pathway. This result is consistent with the observation that ocular growth and emmetropization in Gnat1$^{-/-}$ mice, which lack functional rods, do not respond to FD,[22,23] although the well-known myopia-mitigating effect of strong (photopic) illumination,[45–47] seems to indicate a primary role for cones in emmetropization.

FD per se (excluding any effect of light attenuation) reduced the amount and phosphorylation level of Cx36-IR plaques in the IPL after prolonged treatment (4 weeks), but not after brief treatment (2 days). These results indicate that a decrease in coupling involving Cx36 could be a consequence of FDM, or a factor involved in its progression, rather than a cause of FDM. However, injection of 18-β-GA also reduced the amount of Cx36 and the phosphorylation level of Cx36 in the IPL, indicating that the change in activation of Cx36 is more likely a cause than a consequence of myopia. Furthermore, if the change of Cx36 were a consequence of ocular elongation, it should also be found during LIM; but that was not observed in this study.

The phosphorylation of Cx36 is modulated by neural signaling molecules, including nitric oxide (NO) and dopamine (DA), and by the level of ambient illumination.[11,44] In guinea pigs, FD has been found to reduce retinal DA content,[32] and to transiently suppress retinal NOS activity[47]; thus the dephosphorylation of Cx36 in the IPL could be induced by NO through the cGMP-PKG pathway, or by DA receptors through the cAMP-PKA pathway, and dopamine and NO could affect emmetropization via their regulation of coupling through Cx36-containing GJs. A recent study in mice found that FD by lid-suture for 40 days, which also induces FDM, increased the phosphorylation level of Cx36 in AII amacrines.[26] The discrepancy in effects could be due to factors such as species differences, or the more severe reduction of retinal illumination and alteration of light-spectrum by lid-suturing, which could further enhance Cx36 phosphorylation.[44]

FD and 18-β-GA injections for 4 weeks also decreased the amounts of Cx36 in the IPL, which should further decrease cell-cell coupling. This is consistent with the results of a previous study, which found that FD caused decreased expression of *GJD2* mRNA and Cx36 protein in guinea pig retina.[24] However, in the present study, we also found that HD did not affect the amount of Cx36, and this is inconsistent with a recent report that HD caused decreased expression of *GJD2* mRNA and Cx36 protein in guinea pig retina.[25] In the latter study, LIM was induced with −10 D, which could not be completely compensated after 3 weeks' treatment duration (refraction shifted from 3.64 ± 0.83 to −1.54 ± 0.24). It seems possible that the results in Zhu's study were affected by confounding factors; for example, HD of −10 D might be too much for guinea pigs' retina to recognize as defocus, and instead be effectively processed as unfocused blur.

Our results show that subconjunctival delivery of a nonselective GJ uncoupler, 18-β-GA, enhances myopia development in guinea pigs. In chicks, however, Teves and colleagues reported that intravitreal injection of a Cx35-specific mimetic peptide (Cx35-MP, which is expected to block the assembly of functional GJs) specifically inhibited FDM, in a dose-dependent manner (15th International Myopia Conference, 2015; and W.K. Stell, personal communication); Cx35-MP was also found to enhance contrast sensitivity at higher spatial frequencies.[12] The difference in effects of GJ-uncoupling on emmetropization could be due to differences in rod:cone ratios and rod pathways in these two species (e.g. because the chick retina is cone-dominated, whereas the guinea pig retina is rod-dominated). So far, only mixed rod-cone bipolar cells were identified in the chick retina[48] – as in other non-mammalian species, such as the turtle,[49] in which retinal circuitry is somewhat similar to that in birds.[50] Alternatively, it could be because the Cx35-MP selectively inhibited Cx35-mediated cell-cell coupling in the chicken retina, whereas 18-β-GA (as a nonspecific blocker of coupling) caused myopia through inhibition of other types of GJs, or GJs in tissues other than retina, when injected subconjunctivally in the guinea pig.

The Role of HC-HC Coupling in Emmetropization

FD per se (excluding any effect of light-attenuation) promoted HC-HC coupling (see Fig. 3); therefore, if HC-HC coupling were influential in myopia, blocking HC-HC coupling with 18-β-GA should cause hyperopic shifts. The 18-β-GA attenuated the response to FD; however, whereas 18-β-GA attenuated HC-HC coupling, and the vehicle did not, the drug treatments alone led to myopic rather than hyperopic shifts. These conflicting results suggest that HC-HC coupling, which is known to be mediated by GJs containing Cx57/Cx50 in the mouse,[8,27] might not play a causal role in myopia development. Finally, HD also caused a myopic shift but did not affect HC-HC coupling (see Fig. 3), providing further reasons to question a role for HC-HC coupling in myopia development.

HCs form a wide network of connections through GJs that contain Cx57 and Cx50.[8,26] In rabbit, for example, this extensive network allows HCs to extend their receptive field to at least 25 times that of a single HC.[51,52] In the present study, FD increased tracer coupling among HCs. Considering that FD also reduces the amount of light reaching the eye, we evaluated the HC-HC coupling in animals raised under 40 lux (the same illuminance as transmitted by the diffuser under 300 lux) or 300 lux (the level without diffuser), both of which were in the mesopic to low-photopic range of human vision.[53] Our study showed less coupling under 40 lux than under 300 lux. However, Xin and Bloomfield[9] reported that the degree of coupling was inversely related to light intensity in the rabbit's retina, and the range of light intensity mainly evaluated was from dark adaptation to 3.342 lux (converted from mW/cm^2 to lux, via this website: http://www.egc.com/useful_info_lighting.php); only limited data for the 33.42 to 334.2 lux range were available in Xin's study.[9] In the present study, we found that HC-HC tracer-coupling decreased in the 40 lux group, indicating that the FD-induced increase of HC-HC coupling was due to degradation of images, rather than to a decrease in light level. Subconjunctival injection of 18-β-GA reduced tracer-coupling among HCs, whereas HD did not affect it. This inconsistency in the changes of HC-HC coupling among different myopia models suggests that HC-HC coupling might play only a minor role (or even no role) in the development of myopia in mammals; but the mechanisms might be different in different animal models.

Limitations and Future Directions

The limitations of this study include that 18-β-GA does not act specifically on Cx36, but is expected to affect coupling via GJs composed of many types of connexins.[54,55] It is known the GJs – composed of various connexins

Investigative Ophthalmology & Visual Science

– mediate a variety of cell-cell contacts involving a variety of retinal circuits,[11] which subserve multiple roles with respect to normal vision as well as emmetropization and myopization. Furthermore, GJs are found also in the lens,[38] RPE,[39] choroid,[40] and sclera,[41] and so modulation of coupling by 18-β-GA in any of these locations might well cause changes in axial elongation and refraction. Nevertheless, with these caveats in mind, our results suggest that the functional modulation of Cx36-containing GJs in the retina plays some role in myopia development and emmetropization.

Given that the population of Cx36-containing GJs in the IPL, and the neural circuitry in which they play functional roles, are heterogeneous,[56–58] all of the IHC measurements in this study represent the sum of changes in a heterogeneous population of Cx36-containing GJs. Therefore, regarding the roles of Cx36-containing GJs in FDM or LIM, it is entirely possible that the IF results in FDM and LIM are different simply because these two conditions differentially affect some components of different retinal circuits. It is significant, nevertheless, that this study lays the groundwork for definitive future studies, by providing new background information and suggesting new hypotheses for further testing in the future.

Summary

In this study using a mammalian animal model, we have shown that cell-cell coupling via Cx36-containing GJs in the retina, particularly those in the IPL, can be modulated by FD. This leads to the conclusion that they might play significant roles in emmetropization and myopia development; whereas, in contrast, retinal HC-HC coupling probably plays little or no such roles. These predictions should be tested in further studies.

Acknowledgments

The authors thank John O'Brien (Department of Ophthalmology and Visual Science, the University of Texas Health Science Center, Houston, TX, USA for providing rabbit anti-Cx36 (phospho-Ser293) IgG; and William K. Stell (Department of Cell Biology and Anatomy, University of Calgary, Calgary, Alberta, Canada) for critical reading and editing of the manuscript.

Supported by Grants 81700871, 82025009, 81670876, 81830027, 81970833, and 81790641 from the National Natural Science Foundation of China; and by Grant LY18H120006 from Natural Science Foundation of Zhejiang Province.

Disclosure: **Z. Zhi**, None; **J. Xiang**, None; **Q. Fu**, None; **X. Pei**, None; **D. Zhou**, None; **Y. Cao**, None; **L. Xie**, None; **S. Zhang**, None; **S. Chen**, None; **J. Qu**, None; **X. Zhou**, None

References

1. Holden BA, Fricke TR, Wilson DA, et al. Global prevalence of myopia and high myopia and temporal trends from 2000 through 2050. *Ophthalmology*. 2016;123:1036–1042.
2. Zhou X, Lu F, Xie R, et al. Recovery from axial myopia induced by a monocularly deprived facemask in adolescent (7-week-old) guinea pigs. *Vision Res.* 2007;47:1103–1111.
3. Zheng H, Tse DY, Tang X, To C, Lam TC. The interactions between bright light and competing defocus during emmetropization in chicks. *Invest Ophthalmol Vis Sci.* 2018;59:2932–2943.
4. Xiong S, Sankaridurg P, Naduvilath T, et al. Time spent in outdoor activities in relation to myopia prevention and control: a meta-analysis and systematic review. *Acta Ophthalmologica*. 2017;95:551–566.
5. Wässle H. Parallel processing in the mammalian retina. *Nat Rev Neurosci.* 2004;5:747–757.
6. O'Brien J. The ever-changing electrical synapse. *Curr Opin Neurobiol.* 2014;29:64–72.
7. Kar R, Batra N, Riquelme MA, Jiang JX. Biological role of connexin intercellular channels and hemichannels. *Arch Biochem Biophys.* 2012;524:2–15.
8. Janssen-Bienhold U, Trumpler J, Hilgen G, et al. Connexin57 is expressed in dendro-dendritic and axo-axonal gap junctions of mouse horizontal cells and its distribution is modulated by light. *J Comp Neurol.* 2009;513:363–374.
9. Xin D, Bloomfield SA. Dark- and light-induced changes in coupling between horizontal cells in mammalian retina. *J Comp Neurol.* 1999;405:75–87.
10. Demb JB, Pugh EN. Connexin36 forms synapses essential for night vision. *Neuron.* 2002;36:551–553.
11. Bloomfield SA, Völgyi B. The diverse functional roles and regulation of neuronal gap junctions in the retina. *Nat Rev Neurosci.* 2009;10:495–506.
12. Shi Q, Teves MM, Lillywhite A, Pagtalunan EB, Stell WK. Light adaptation in the chick retina: dopamine, nitric oxide, and gap-junction coupling modulate spatiotemporal contrast sensitivity. *Exp Eye Res.* 2020;195:108026.
13. Zhou X, Pardue MT, Iuvone PM, Qu J. Dopamine signaling and myopia development: What are the key challenges. *Prog Retin Eye Res.* 2017;61:60–71.
14. Carr BJ, Stell WK. Nitric oxide (NO) mediates the inhibition of form-deprivation myopia by atropine in chicks. *Sci Rep.* 2016;6:9.
15. Seko Y, Shimizu M, Tokoro T. Retinoic acid increases in the retina of the chick with form deprivation myopia. *Ophthalmic Res.* 1998;30:361–367.
16. Völgyi B, Kovács-Öller T, Atlasz T, Wilhelm M, Gábriel R. Gap junctional coupling in the vertebrate retina: variations on one theme? *Prog Retin Eye Res.* 2013;34:1–18.
17. Mills SL, O'Brien JJ, Li W, O'Brien J, Massey SC. Rod pathways in the mammalian retina use connexin 36. *Prog Retin Eye Res.* 2001;436:336–350.
18. Feigenspan A, Janssen-Bienhold U, Hormuzdi S, et al. Expression of connexin36 in cone pedicles and OFF-cone bipolar cells of the mouse retina. *J Neurosci.* 2004;24:3325–3334.
19. O'Brien JJ, Chen X, Macleish PR, O'Brien J, Massey SC. Photoreceptor coupling mediated by connexin36 in the primate retina. *J Neurosci.* 2012;32:4675–4687.
20. Meguro A, Yamane T, Takeuchi M, et al. Genome-wide association study in Asians identifies novel loci for high myopia and highlights a nervous system role in its pathogenesis. *Ophthalmology.* 2020; 127:1612–1624.
21. Verhoeven VJ, Hysi PG, Wojciechowski R, et al. Genome-wide meta-analyses of multiancestry cohorts identify multiple new susceptibility loci for refractive error and myopia. *Nat Genet.* 2013;45:314–318.
22. Umino Y, Solessio E, Barlow RB. Speed, spatial, and temporal tuning of rod and cone vision in mouse. *J Neurosci.* 2008;28:189–198.
23. Park H, Jabbar SB, Tan CC, et al. Visually-driven ocular growth in mice requires functional rod photoreceptors. *Invest Ophthalmol Vis Sci.* 2014;55:6272–6279.
24. Yang GY, Liu FY, Li X, Zhu QR, Chen BJ, Liu LQ. Decreased expression of gap junction delta-2 (GJD2) messenger RNA and connexin 36 protein in form-deprivation myopia of guinea pigs. *Chin Med J.* 2019;132:1700–1705.
25. Zhu Q, Yang G, Chen B, Liu F, Li X, Liu L. Altered expression of GJD2 messenger RNA and the coded protein connexin 36

Investigative Ophthalmology & Visual Science

in negative lens-induced myopia of guinea pigs. *Optom Vis Sci.* 2020;97:1080–1088.
26. Banerjee S, Wang Q, Zhao F, et al. Increased connexin36 phosphorylation in AII amacrine cell coupling of the mouse myopic retina. *Front Cell Neurosci.* 2020;14:124.
27. Dorgau B, Herrling R, Schultz K, et al. Connexin50 couples axon terminals of mouse horizontal cells by homotypic gap junctions. *J Comp Neurol.* 2015;523:2062–2081.
28. Troilo D, Smith EL, 3rd, Nickla DL, et al. IMI - Report on experimental models of emmetropization and myopia. *Invest Ophthalmol Vis Sci.* 2019;60:M31–M88.
29. Kovács-Öller T, Debertin G, Balogh M, et al. Connexin36 expression in the mammalian retina: a multiple-species comparison. *Front Cell Neurosci.* 2017;11:65.
30. Choi HJ, Ribelayga CP, Mangel SC. Cut-loading: a useful tool for examining the extent of gap junction tracer coupling between retinal neurons. *J Vis Exp.* 2012;12:3180.
31. Lu F, Zhou X, Zhao H, et al. Axial myopia induced by a monocularly-deprived facemask in guinea pigs: a non-invasive and effective model. *Exp Eye Res.* 2006;82:628–636.
32. Dong F, Zhi Z, Pan M, et al. Inhibition of experimental myopia by a dopamine agonist: different effectiveness between form deprivation and hyperopic defocus in guinea pigs. *Mol Vis.* 2011;17:2824–2834.
33. El-Nimri NW, Wildsoet CF. Effects of topical latanoprost on intraocular pressure and myopia progression in young guinea pigs. *Invest Ophthalmol Vis Sci.* 2018;59:2644–2651.
34. Zhang S, Yang J, Reinach PS, et al. Dopamine receptor subtypes mediate opposing effects on form deprivation myopia in pigmented guinea pigs. *Invest Ophthalmol Vis Sci.* 2018;59:4441–4448.
35. Cheng ZY, Wang XP, Schmid KL, Han XG. Inhibition of form-deprivation myopia by a GABAAOr receptor antagonist, (1,2,5,6-tetrahydropyridin-4-yl) methylphosphinic acid (TPMPA), in guinea pigs. *Graefes Arch Clin Exp Ophthalmol.* 2014;252:1939–1946.
36. Li H, Zhang Z, Blackburn MR, Wang SW, Ribelayga CP, O'Brien J. Adenosine and dopamine receptors coregulate photoreceptor coupling via gap junction phosphorylation in mouse retina. *J Neurosci.* 2013;33:3135–3150.
37. Peichl L, González-Soriano J. Morphological types of horizontal cell in rodent retinae: a comparison of rat, mouse, gerbil, and guinea pig. *Vis Neurosci.* 1994;11:501–517.
38. Mathias RT, White TW, Gong X. Lens gap junctions in growth, differentiation, and homeostasis. *Physiol Rev.* 2010; 90: 179–206.
39. Danesh-Meyer HV, Zhang J, Acosta ML, Rupenthal ID, Green CR. Connexin43 in retinal injury and disease. *Prog Retin Eye Res.* 2016;51:41–68.
40. De Stefano ME, Mugnaini E. Fine structure of the choroidal coat of the avian eye. Vascularization, supporting tissue and innervation. *Anat Embryol (Berl).* 1997;195:393–418.
41. Raviola G, Sagaties MJ, Miller C. Intercellular junctions between fibroblasts in connective tissues of the eye of macaque monkeys. A thin section and freeze fracture analysis. *Invest Ophthalmol Vis Sci.* 1987;28:834–841.
42. Guldenagel M, Ammermüller J, Feigenspan A, et al. Visual transmission deficits in mice with targeted disruption of the gap junction gene connexin36. *J Neurosci.* 2001;21:6036–6044.
43. Lee EJ, Han JW, Kim HJ, et al. The immunocytochemical localization of connexin 36 at rod and cone gap junctions in the guinea pig retina. *Eur J Neurosci.* 2003;18:2925–2934.
44. Kothmann WW, Massey SC, O'Brien J. Dopamine-stimulated dephosphorylation of connexin 36 mediates AII amacrine cell uncoupling. *J Neurosci.* 2009;29:14903–14911.
45. Chakraborty R, Yang V, Park HN, et al. Lack of cone mediated retinal function increases susceptibility to form-deprivation myopia in mice. *Exp Eye Res.* 2019;180:226–230.
46. Li W, Lan W, Yang S, et al. The effect of spectral property and intensity of light on natural refractive development and compensation to negative lenses in guinea pigs. *Invest Ophthalmol Vis Sci.* 2014;55:6324–6332.
47. Ashby R, Ohlendorf A, Schaeffel F. The effect of ambient illuminance on the development of deprivation myopia in chicks. *Invest Ophthalmol Vis Sci.* 2009;50:5348–5354.
48. Günther A, Dedek K, Haverkamp S, Irsen S, Briggman KL, Mouritsen H. Double cones and the diverse connectivity of photoreceptors and bipolar cells in an avian retina. *J Neurosci.* 2021;41(23):5015–5028.
49. Dacheux RF. Connections of the small bipolar cells with the photoreceptors in the turtle. An electron microscope study of Golgi-impregnated, gold-toned retinas. *J Comp Neurol.* 1982;205:55–62.
50. Mariani AP. Neuronal and synaptic organization of the outer plexiform layer of the pigeon retina. *Am J Anat.* 1987;179:25–39.
51. Bloomfield SA, Miller RF. A physiological and morphological study of the horizontal cell types of the rabbit retina. *J Comp Neurol.* 1982;208:288–303.
52. Bloomfield SA, Xin D, Persky SE. A comparison of receptive field and tracer coupling size of horizontal cells in the rabbit retina. *Vis Neurosci.* 1995;12:985–999.
53. Grimes WN, Songco-Aguas A, Rieke F. Parallel processing of rod and cone signals: retinal function and human perception. *Annu Rev Vis Sci.* 2018;4:123–141.
54. Pan F, Mills SL, Massey SC. Screening of gap junction antagonists on dye coupling in the rabbit retina. *Vis Neurosci.* 2007;24:609–618.
55. Guan X, Wilson S, Schlender KK, Ruch RJ. Gap-junction disassembly and connexin 43 dephosphorylation induced by 18 beta-glycyrrhetinic acid. *Mol Carcinog.* 1996;16:157–164.
56. Bloomfield SA, Volgyi B. Function and plasticity of homologous coupling between AII amacrine cells. *Vis Res.* 2004;44:3297–3306.
57. Pan F, Paul DL, Bloomfield SA, Volgyi B. Connexin36 is required for gap junctional coupling of most ganglion cell subtypes in the mouse retina. *J Comp Neurol.* 2010;518:911–927.
58. Telkes I, Kobor P, Orban J, Kovacs-Oller T, Volgyi B, Buzas P. Connexin-36 distribution and layer-specific topography in the cat retina. *Brain Struct Funct.* 2019;224:2183–2197.

Investigative Ophthalmology & Visual Science